Chapter 4

Nonlinear System Identification Using Frequency Domain Data

A dynamic model is usually a mathematical, simplified description of a true system. Input-output modeling, by its name, aims to construct an abstract model description from the input and output data of a real system. System identification is a well-studied field about techniques to identify model structures, estimate parameters and validate models. The literature on system identification is extensive [God93, Hsi77, Lju94, Lju99, Nor86, Unb87, Wal82]. There are a large number of techniques and methods to systematically identify systems in both the time-domain and the frequency domain, and also many works focused on modeling and identification in various application areas. These methods are mainly on linear system identification. For nonlinear system identification, one approach is to use "black box" models such as neural networks or fuzzy logic techniques [Mas93]. A more systematic analysis is to build a model in the form of nonlinear differential equations or Volterra series. Applying an appropriate perturbation signal, such as random noise or a pseudo-random binary signal (PRBS) as input, the nonlinear response of the system is obtained [God93]. With spectrum analysis tools, nonlinear system identification can also be performed using signal correlations [Ben90]. In the field of structural mechanics, nonlinear system parameters can be estimated with harmonic response data based on the known mode shapes of the structure [Yas89, Yas97]. The advantage of identification of a nonlinear system in the frequency domain is disturbance or noise rejection due to selective choosing of only significant signal frequency data and ignoring noises spectrum.

In the section, we review input-output modeling with emphasis on nonlinear systems. Both nonlinear differential equation and state-space model structures are

studied. To meet the needs of this work, a frequency domain nonparametric nonlinear system identification technique based on harmonic balancing theory is proposed and developed. Applying this identification technique, one can obtain a nonlinear model from input output data in frequency domain. A discussion of the nonuniqueness of state-space model representation is also presented, and a recursive identification algorithm for state-space modeling is formally developed. An example of Hammerstein-Wiener model identification is also provided. Furthermore, as an example of actual nonlinear system identification, a nonlinear heat release model is successfully developed with a combination of linear modeling and nonlinear system identifications techniques based on nonlinear frequency response data from laminar premixed flame experiments. The challenges and limitations of this approach are also discussed.

4.1 **Input-Output Modeling**

The fundamental ideal of input-output modeling is to build a model from input output simulation or experimental data. It normally is used on complicated systems, where the first-principles models are too complicated, the structure of the system is very hard to model mathematically, and the intermediate state variables are not accessible or are extremely difficult to measure. With only input output data information, a model structure must be defined, parameterized and identified. It is also frequently referred as a nonparametric identification problem since they do not have a confined set of possible models defined. There are many ways to describe models for a dynamic system. For linear time invariant (LTI) systems, the most common system models are transfer functions, which are the Laplace transformation of underlying differential equations, and state-spaced models [Bay98]. These models apply to continuous time as well as discrete time systems, with necessary changes from the *s*-domain to the *z*-domain, or from differential equations to difference equations.

Nonlinear systems can be modeled by nonlinear differential equations and state space realizations. Given a nonlinear system, linearization at an equilibrium point gives a linear model that characterizes the small perturbation response of the system. It is

important to choose an appropriate structure for the model before applying an identification procedure. Experience shows that when the basic structure of the system is correct, it will not take too much time to fine tune the order of the system and search for a best fit to the data. For nonlinear systems, as we will discuss in the following sections, the form of nonlinearity and structure of the model are remarkably significant.

4.1.1 Model by Differential Equations

An n^{th} order, continuous time, linear time invariant system has transfer function $G(s)$ given by,

$$G(s) = \frac{b_m s^m + b_{m-1} s^{m-1} + \cdots + b_2 s^2 + b_1 s + b_0}{a_n s^n + a_{n-1} s^{n-1} + \cdots + a_2 s^2 + a_1 s + a_0} \tag{4.1}$$

Usually, a_n is set to 1. Alternatively, a LTI system can be represented by a differential equation with input u and output y as,

$$y^{(n)} = -a_{n-1} y^{(n-1)} - \cdots - a_2 \ddot{y} - a_1 \dot{y} - a_0 y + b_m u^{(m)} + b_{m-1} u^{(m-1)} + \cdots + b_2 \ddot{u} + b_1 \dot{u} + b_0 u \tag{4.2}$$

To identify a linear system in the time domain from the differential equation above, a finite difference method can be used to approximate the derivatives. Using the data recorded at each time step, the m+n+1 coefficients can be obtained by parameter estimation algorithms.

An n^{th} order non-autonomous nonlinear system can be represented as,

$$y^{(n)} = f(y^{(n-1)}, \cdots, \ddot{y}, \dot{y}, y, u^{(m)}, u^{(m-1)}, \cdots, \ddot{u}, \dot{u}, u, \theta) \tag{4.3}$$

where θ is the collection of coefficients for the linear and nonlinear terms. This is a natural extension of the linear differential equation. Many techniques are available for the

analysis of weakly nonlinear systems, e.g. perturbation methods, multiple scales, generalized method of averaging, and etc [Nay81]. Nonlinear system dynamics has been studied extensively, usually for very simple nonlinear differential equations. Nonlinear responses are far more varied and complicated than the response of linear systems. Investigation of bifurcation maps, multifrequency excitations, amplitude jumps, frequency shifts and chaos are used to gain knowledge of nonlinear systems [Nay93]. Nonlinear identification has received less attention.

4.1.2 State-Space Nonlinear Model and Realizations

The state space representation of a LTI system has various forms of realizations, but it can always be described in the form of,

$$\begin{aligned} \dot{x} &= Ax + Bu \\ y &= Cx + Du \end{aligned} \tag{4.4}$$

Here, x is the state vector, u is the input and y is the system output. The transformation between state space model and transfer function $G(s)$ is,

$$G(s) = C(sI - A)^{-1}B + D \tag{4.5}$$

As we know, the state space model of a linear system is not unique. With a transformation matrix M, the formal state space model can be transformed into a different set of system matrices $\{A, B, C, D\}$. Controllable and observable realizations are normally considered for linear system identification.

For nonlinear systems, the state and output equation can be described as,

$$\begin{aligned} \dot{x} &= f(x,u) \\ y &= g(x,u) \end{aligned} \tag{4.6}$$

where $f(x, u)$ and $g(x, u)$ are nonlinear functions. We can obtain a linearized model at any equilibrium point and the Jacobian matrix is used to determine local stability. Unlike a SISO linear system model, where there is always a global transformation from state space form to an input-output differential equation, a SISO nonlinear state space description, such as equation (4.6), may not always be able to be transformed into a nonlinear input-output differential equation, such as equation (4.3), over the entire space.

4.2 Nonlinear System Identification

In contrast to linear system identification, the nonlinear problem brings many more difficulties. In this section, we first review the generalized system identification techniques with simple examples. The practical side of nonlinear system identification is then discussed. With an example of 2nd order weakly nonlinear flame model that we developed earlier, we discuss in details that input-output differential equation may not have solutions for certain system description.

4.2.1 Overview of nonlinear system identification techniques

Analogous to linear system identification, nonlinear system identification can be classified into time domain and frequency domain methods. With data collected in time series, time domain method is useful for discrete time nonlinear systems. As for the frequency domain method, it is applied with input-output spectrum data. It can be implemented with correlation method, harmonic balancing, stochastic modeling and etc.

Meanwhile, nonlinear system identification techniques can also be categorized as parametric and nonparametric. For specific applications, physical study sometimes unveils the nonlinearity of the system, or suggests the basic structure of the model. Under certain circumstances with known or assumed nonlinearity, parametric identification is applied to estimate all linear and nonlinear parameters using pseudo-linear regression, LS, RLS, nonlinear instrumental variables, or prediction-correction methods. For a system with unknown nonlinearities, which may be embedded among several complicated partial differential equations such as flame dynamics, nonparametric

identification prevails. It uses a functional expansion technique to approximate the unknown nonlinearity $f(x)$, and it is often referred to as nonlinear mapping. It maps the nonlinearity with a set of basis functions $P_n(x)$. The coefficient of each basis function is subsequently estimated to find the model best fitting the data.

The fundamental ideal of nonlinear mapping is to choose a set of basis functions that can approximate any arbitrary function with a sufficiently large number of terms. There is abundant literature available on approximation theory [Zie81][Dan71][Hro87] [Dan78]. Traditional functional expansions consist of orthogonal polynomial expansions to minimize the error $\int_a^b [f(x) - P_n(x)]dx$. For a single variable, Taylor series expansion, $P_n(x) = a_n x^n + a_{n-1} x^{n-1} + \cdots + a_1 x + a_0$, is widely used. Chebychev polynomials are also widely used, because of their orthogonality on the interval [-1, 1]. Fourier series expansion is considerably useful in conjunction with frequency domain identification, and the expansion is given by,

$$P_n(x) = \frac{a_0}{2} + \sum_{k=1}^{n-1} (a_k \cos kx + b_k \sin kx).$$

Padé approximation extends the ideal of polynomial expansion to rational functions using,

$$P_n(x) = \frac{p(x)}{q(x)} = \frac{p_0 + p_1 x + \cdots + p_n x^n}{q_0 + q_1 x + \cdots + q_m x^m} \tag{5.9}$$

Additionally, spline and piecewise linear approximation can approximate nonlinear functions well. A classic approximation difficulty among polynomial expansion technique is large error at the boundaries of the approximation region. Splines have better boundary properties, but the disadvantage is lack of a closed form and too many coefficients.

Now, we review two classes of identification algorithms that can be used with parametric as well as nonparametric identification. The pseudo-linear regression with weighted least squares (WLS) method is recommended as an initial trial for parameter estimation. A practical example of pseudo-linear regression is applying it to the second order numerical flame model that we obtained in section 3.3. The second nonlinear flame model can be described as,

$$\begin{bmatrix} \dot{a}_1 \\ \dot{a}_2 \end{bmatrix} = \begin{bmatrix} f_1(a_1, a_2, u) \\ f_2(a_1, a_2, u) \end{bmatrix} \qquad (4.10)$$
$$y = f(a_1, a_2)$$

Through numerical simulation, a complete set of data for each input, output and state variable pair is obtained if the state variables are observable. Assume the nonlinearity of the state equations and the output equations is static, and it can be approximated by a set of quadratic and cubic nonlinear terms. For the state equation, the linear term are given by a_1, a_2, u, and the quadratic nonlinear terms are given by $a_1^2, a_2^2, a_1a_2, a_1u, a_2u, u^2$, and the cubic nonlinear terms are given by $a_1^3, a_2^3, u^3, a_1a_2^2, a_1^2a_2, a_1u^2, a_2u^2, a_1a_2u, a_1^2u, a_2^2u$. The unknown coefficients for functions f_1 and f_2 are listed individually as in column vectors θ1 and θ_2.

$$\theta_1 = \begin{bmatrix} \alpha_1 & \alpha_2 & \cdots & \alpha_{19} \end{bmatrix}^T, \theta_2 = \begin{bmatrix} \beta_1 & \beta_2 & \cdots & \beta_{19} \end{bmatrix}^T.$$

With data collected at each time t_i, the state equation can be formulated as,

$$Y_p = \begin{bmatrix} \dot{a}_1(t_1) & \dot{a}_1(t_2) & \cdots & \dot{a}_1(t_n) \\ \dot{a}_2(t_1) & \dot{a}_2(t_2) & \cdots & \dot{a}_2(t_n) \end{bmatrix}^T, \qquad (4.11)$$

$$A_p = \begin{bmatrix} a_1(t_1) & \cdots & a_1^2(t_1) & \cdots & a_1^3(t_1) & \cdots \\ a_1(t_2) & \cdots & a_1^2(t_2) & & a_1^3(t_2) & \cdots \\ \vdots & \vdots & \vdots & \vdots & \vdots & \vdots \\ a_1(t_n) & \cdots & a_1^2(t_n) & & a_1^3(t_n) & \cdots \end{bmatrix} \qquad (4.12)$$

Therefore, $Y_p = A_p\theta + \nu_p$, where v_p represents the model error, and θ is the collection of coefficients given by $\theta = [\theta_1 \quad \theta_2]$. Linear regression with weighting matrix W gives solution,

$$\hat{\theta} = (A_p^T W A_p)^{-1} A_p^T W Y_p \tag{4.13}$$

Thus, all the unknown coefficients can be determined by WLS method as in (4.13). The output equation can be formulated and solved in the same way. Figure 4.1 and Figure 4.2 show that the approximation of the state functions and output function are well matched using the linear regression approach. Overall, pseudo-linear regression is an easy yet effective approach to estimate model parameters.

However, not all parameter estimation problems can be solved by linear regression. Nonlinear regression algorithms are well established as a general approach to obtain nonlinear parameters. The Gauss-Newton method and Levenberg-Marquardt method are two algorithms that are commonly applied.

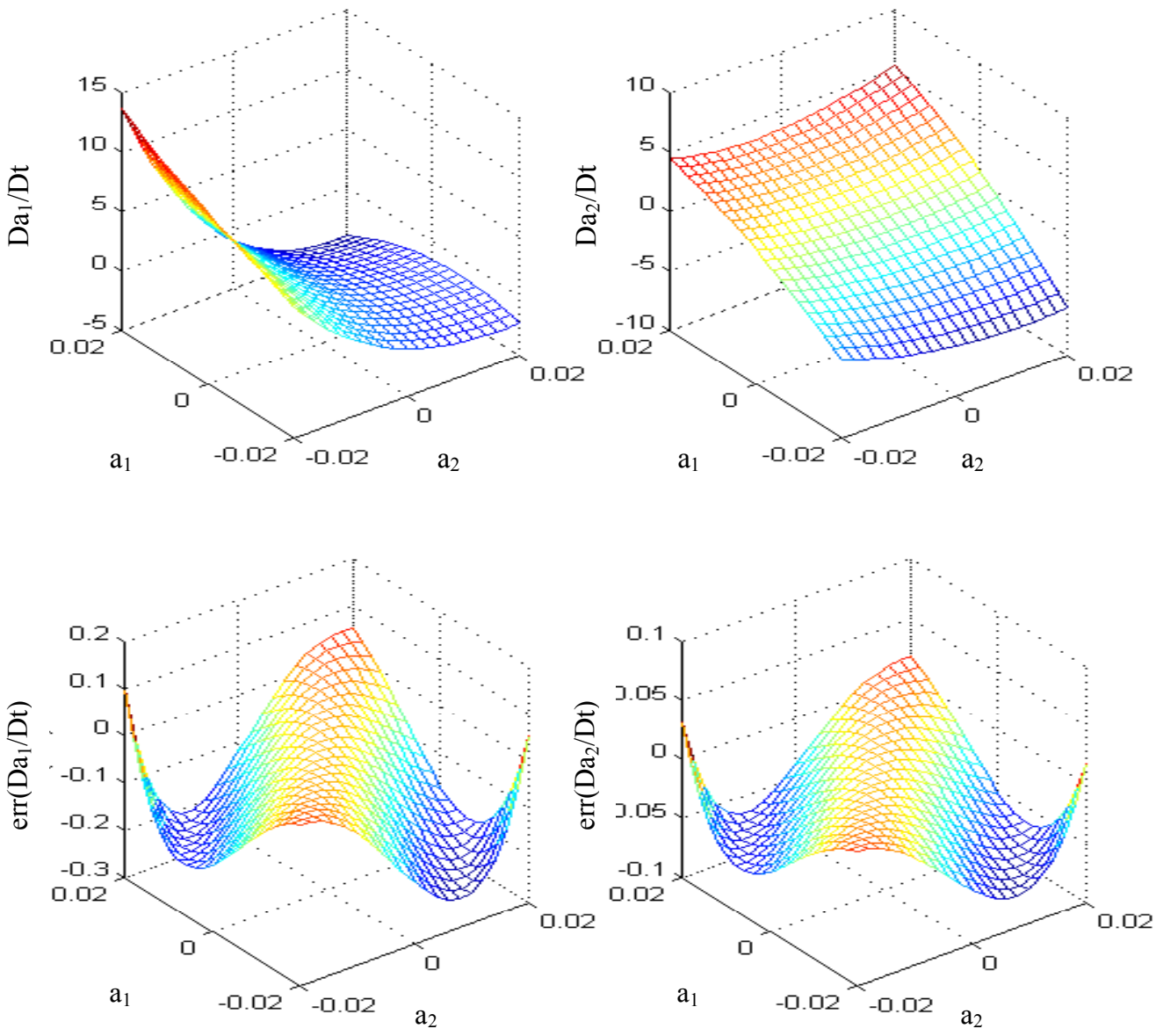

Figure 4.1 Approximation results of state equations

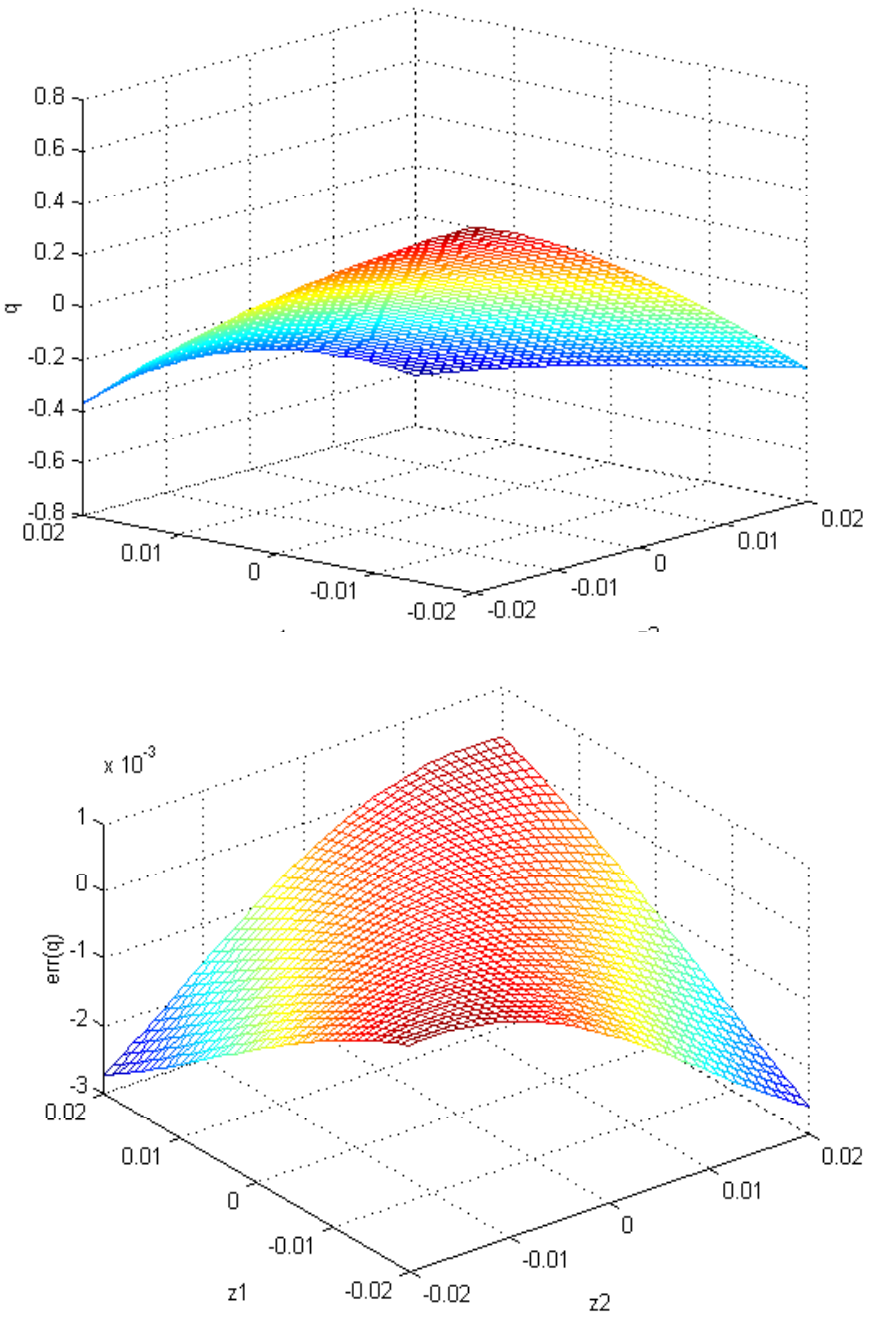

Figure 4.2 Approximation result of output equation

As an example of a nonlinear parameter estimation problem, consider a simplified one step reaction with reaction rate in Arrhenius form that can be expressed as,

$$\frac{d[CH_4]}{dt} = AT^b \exp(-E_A / R_u T)[CH_4]^m [O_2]^n \qquad (4.14)$$

Assuming the reaction rate, temperature as well as fuel and oxygen mole concentrations are available, the goal is to find a proper pre-exponential factor A, activation energy E_A, and all exponents m, n, b. A straight logarithmic transformation cannot reformulate this problem as a linear regression problem. So, nonlinear regression with a parameter optimization algorithm is necessary for this parameter approximation problem.

As an additional resource, black box models using neural networks, wavelets, or fuzzy logic are also powerful modeling tools in the system identification field. Figure 4.3 shows a diagram of a black box model using a neural network.

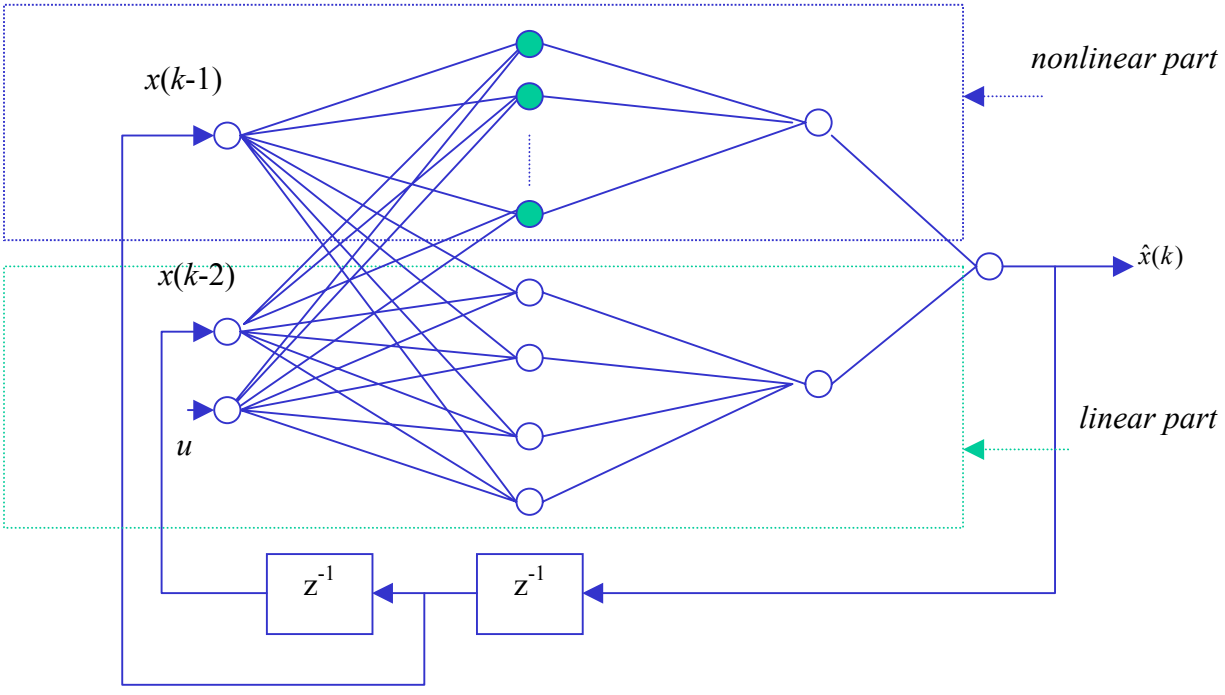

Figure 4.3 An example of neural network black box model

4.2.2 The practical side of nonlinear system identification

Practical system identification begins with experiment design or numerical simulation to collect the data that we will use it to identify a system. This is followed by choosing a model structure, applying functional expansion to approximate the nonlinearity, and then implementing regression or optimization algorithms to estimate the parameters.

The original data sets from experiments or simulation are very important. The designed experiments should excite all necessary conditions and contain all dynamics that we are interested in and which eventually will be expressed in the identified model. To identify a system in the time domain, a large amount of data may be needed, and the noise level must be considered. In the frequency domain, one must be careful if the actual input is fed back from the output, since spectral and correlation analysis may not be reliable.

The perturbation signal is an important aspect of system identification. It is necessary to choose a proper input signal to the system so the measured output reflects all the dynamics needed. With a well-designed perturbation signal, this could reduce the amount of data collected and increase the accuracy of the parameter estimate. Generally, a pseudo-random binary input or a band-limited white noise input has the nice property of a flat spectrum, and they are good for weakly nonlinear system identification. Figure 4.4 displays a binary PN sequence and its spectrum.

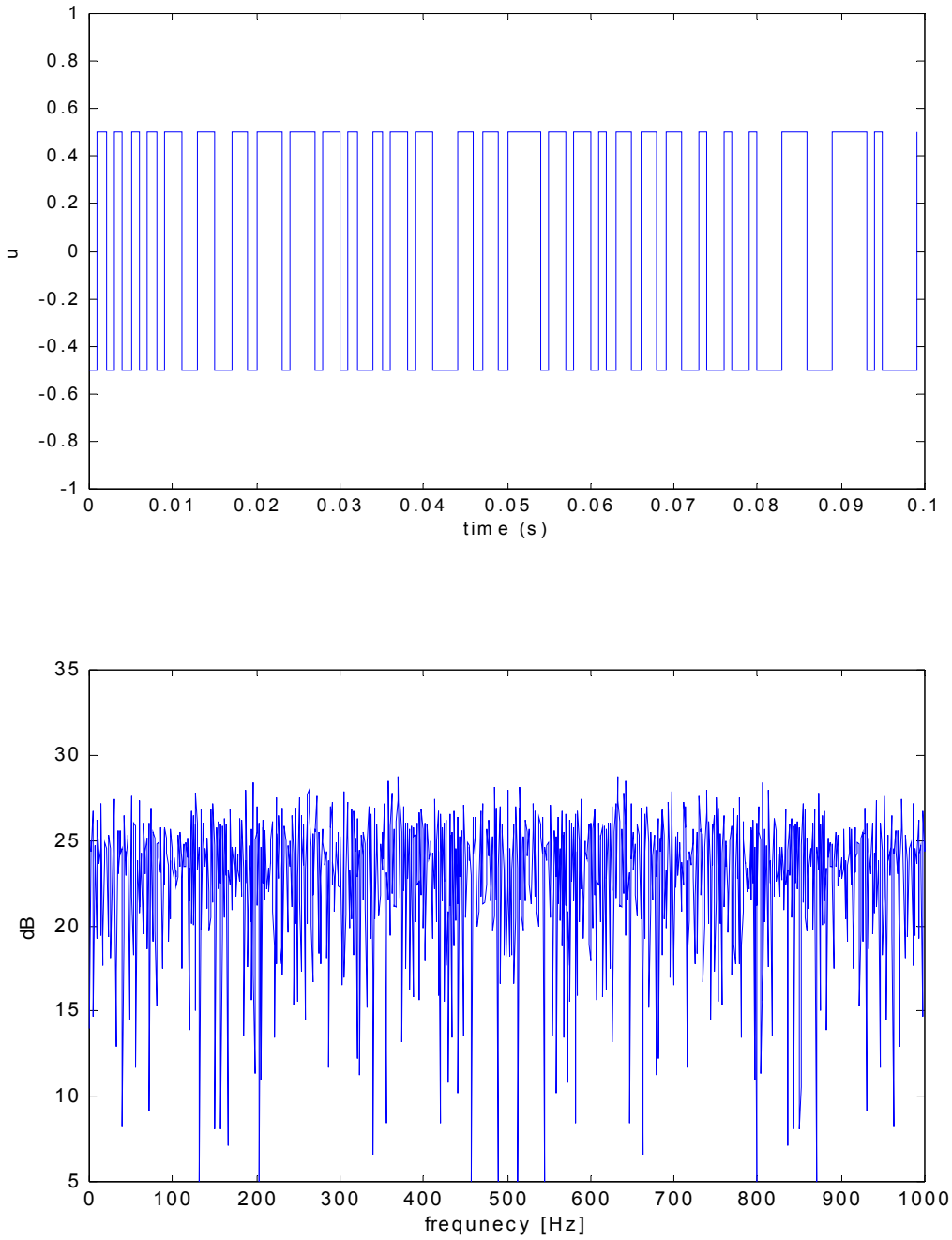

Figure 4.4 Binary pseudo-random perturbation signal and spectrum

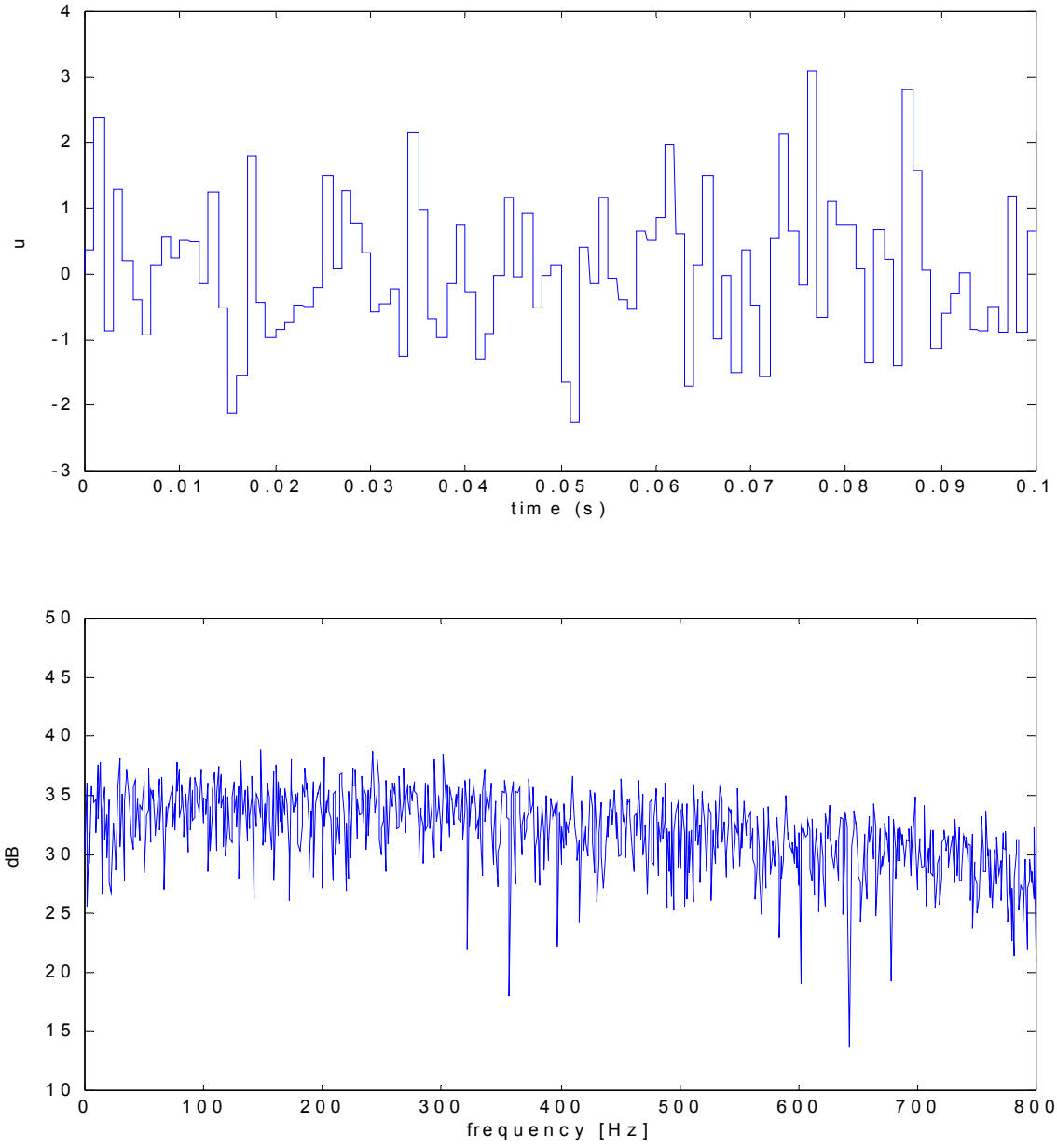

Figure 4.5 Band-limited white noise signal and spectrum

An example of band-limited white noise and its spectrum is shown in Figure 4.5. Bendat et. al. developed a system identification procedure using a random input and spectrum correlations [Ben90]. However, these two random perturbation signals do not fit all cases. For instance, to identify large signal nonlinear dynamics requires the input signal to not only cover the relevant frequency band but also all relevant amplitudes. A describing function technique would be a more effective approach, and we will discuss it in Chapter 5 in detail.

Another major difficulty is multivariable nonlinear mapping for some applications where physical insight may be lacking or it is difficult to come up with structured nonlinearities on physical grounds. For SISO nonlinear systems, this is often related to the order of the model. For an *n*th order differential equation (4.3), there are *2n* linear parameters: $y^{(n)}$, $\cdots$, $\dot{y}$, y, $u^{(n)}$, $\cdots$, $\dot{u}$, u. A polynomial expansion could list n^2 quadratic terms, n^3 cubic terms, and the number of terms goes exponentially as the order of nonlinear terms increases. For a multi-input multi-output system, the difficulty of nonlinearity approximation and the number of polynomial terms is even worse. As the number of terms increases, the result will fit the data better. However, a model with a huge number of terms is useless. Indeed, as the number of nonlinear terms gets larger, stability of the system becomes hard to enforce. The idea of subsystem identification will be proposed and developed with an example in section 4.4.2. The basic principle is "divide-and-conquer", to split the original model into subsystems considering the model structure. Each subsystem can be identified individually with far fewer terms. This technique avoids a large number of nonlinear terms, the high order model problem, and eases the stability study of the identified nonlinear system.

This brings us back to the discussion of the amount of data needed for identification. Assuming an nth order nonlinear system is in the form of equation (4.3), and there are 2*n* parameters, $y^{(n)}$, $\cdots$, $\dot{y}$, y, $u^{(n)}$, $\cdots$, $\dot{u}$, u, that need to be measured while generating data sets. This is equivalent to a 2*n*-dimensional approximation problem. Ideally, we could discretize each dimension using *m* points, and

this would result m^{2n} data sets. For a 10th order model, if each dimension has 10 discrete points, the number of data sets needed to cover the space is 10^{20}! It is virtually impossible to generate this amount of data and map a function to fit it. Note that for a linear system you would only need 20 points to determine the required function.

4.2.2.1 Input-output differential equation form may not have solution

For experimental identification, only the input and output are typically be measured. The obvious choice for a model structure is an input-output differential equation of the form,

$$q^{(n)} = f(q^{(n-1)}, \cdots, \ddot{q}, \dot{q}, q, u^{(m)}, u^{(m-1)}, \cdots, \ddot{u}, \dot{u}, u) \tag{4.15}$$

Unfortunately, this structure may not always be able to model the flame over a sufficiently large region. We show below that over the nonlinear ODE models that have been constructed in Chapter 3 cannot be put into the form of (4.15) globally.

For the purpose of graphical interpretation, we consider the simple 2nd order weakly nonlinear state space model that we developed for the small perturbation response of flame dynamics as an example. As we mentioned earlier, for small perturbations there are two dominant modes for the heat release dynamics. x_1 and x_2 are state variables, the multipliers for the two modal functions.

$$\begin{bmatrix} \dot{x}_1 \\ \dot{x}_2 \end{bmatrix} = \begin{bmatrix} f_1(x_1, x_2, u, \theta_1) \\ f_2(x_1, x_2, u, \theta_2) \end{bmatrix} \tag{4.16}$$
$$q = g(x_1, x_2)$$

For the 2nd order state space model above, is it possible to convert it into an input-output differential equation, such as,

$$\ddot{q} = h(\dot{q}, q, \dot{u}, u, \theta) \ ? \tag{4.17}$$

Equation (4.16) can be differentiated to yield,

$$
\begin{aligned}
q &= g(x_1, x_2) \\
\dot{q} &= \frac{\partial g}{\partial x_1} f_1 + \frac{\partial g}{\partial x_2} f_2 = \psi_1(x_1, x_2, u)
\end{aligned}
\tag{4.18}
$$

$$
\begin{aligned}
\ddot{q} &= \frac{\partial^2 g}{\partial x_1^{\,2}} f_1^{\,2} + \frac{\partial g}{\partial x_1} \ddot{x}_1 + \frac{\partial^2 g}{\partial x_2^{\,2}} f_2^{\,2} + \frac{\partial g}{\partial x_2} \ddot{x}_2 \\
&= \frac{\partial^2 g}{\partial x_1^{\,2}} f_1^{\,2} + \frac{\partial g}{\partial x_1}\left(\frac{\partial f_1}{\partial x_1} f_1 + \frac{\partial f_1}{\partial x_2} f_2 + \frac{\partial f_1}{\partial u}\dot{u}\right) + \frac{\partial^2 g}{\partial x_2^{\,2}} f_2^{\,2} + \frac{\partial g}{\partial x_2}\left(\frac{\partial f_2}{\partial x_1} f_1 + \frac{\partial f_2}{\partial x_2} f_2 + \frac{\partial f_2}{\partial u}\dot{u}\right) \\
&= \psi_2(x_1, x_2, u, \dot{u})
\end{aligned}
\tag{4.19}
$$

Equation (4.18) can be used to solve for x_1 and x_2 in terms of q, $\dot{q}$ and u. Substituting into equation (4.19), the differential equation form in (4.17) can be obtained. However, there are interesting problems here while solving for (x_1, x_2) for any $(u, q, \dot{q})$ during the former step. Figure 4.6 shows the contour plot of x_1, x_2 in $(q, \dot{q})$ plane where u is set to 0. In one region of $(q, \dot{q})$ space, there exists multiple intersections of x_1 contours, and a similar situation holds for x_2. Numerically, for certain $(q, \dot{q})$ values, with u set to 0, there are multiple x_1 and x_2 solutions while solving for (x_1, x_2) from equation (4.18). This implies that state variables (x_1, x_2) cannot be uniquely determined from $(u, q, \dot{q})$. Consequently it is not be able to substitute into equation (4.19), and the transformation from state space form into differential equation form breaks down.

Another way to see the problem is by varying $\dot{q}$ holding $u = 0, \dot{u} = 0, q = 0.8$. The state variables ($x_1$, x_2) can be computed from (4.18) by a nonlinear solver. To capture the multiple (x_1, x_2) solutions for each case, the initial solutions are covered within all physically possible range of all (x_1, x_2) values. Then $\ddot{q}$ can be computed from (4.19), and Figure 4.7 demonstrates that there are multiple $\ddot{q}$ possible for a specific $(\dot{q}, q, \dot{u}, u)$. Therefore, this system cannot be described in the form of a 2nd order input-output differential equation.

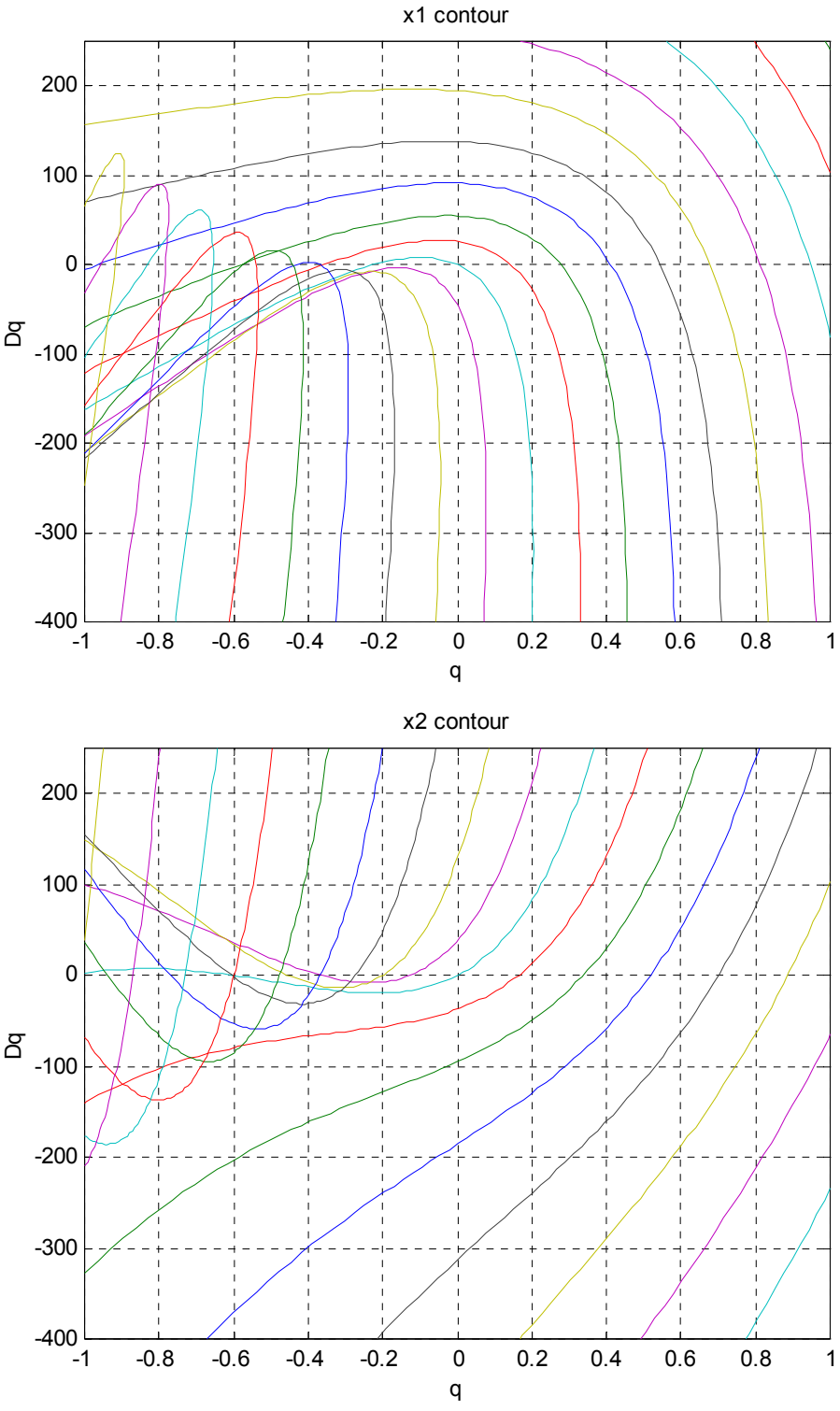

Figure 4.6. Contour plot of x_1, x_2

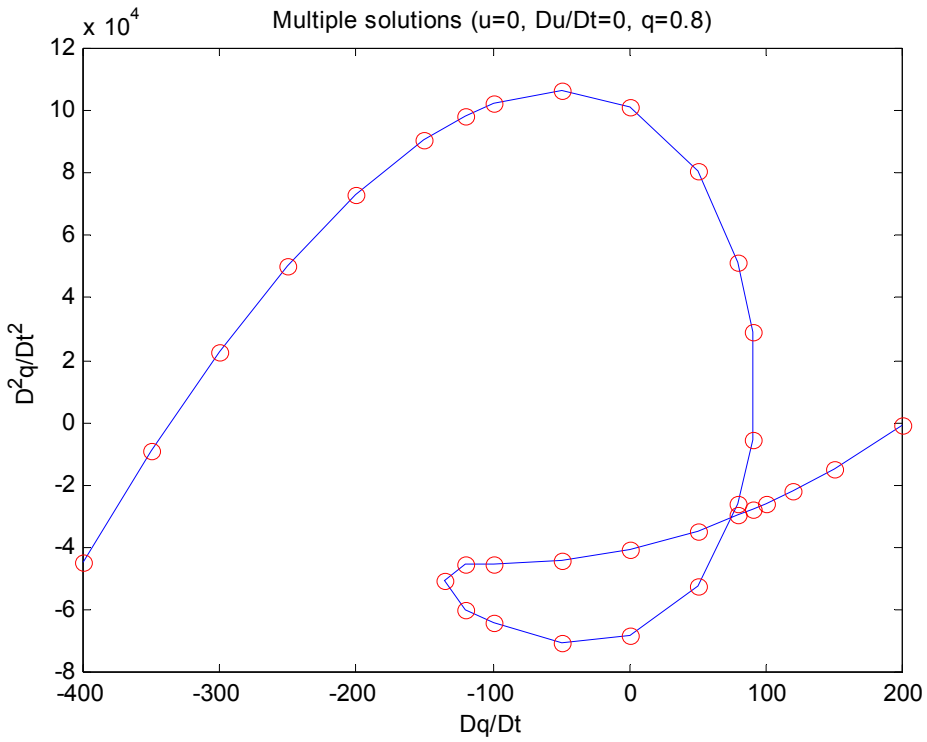

Figure 4.7. A plot of $\ddot{q} - \dot{q}$ with constant setting $(q, u, \dot{u})$

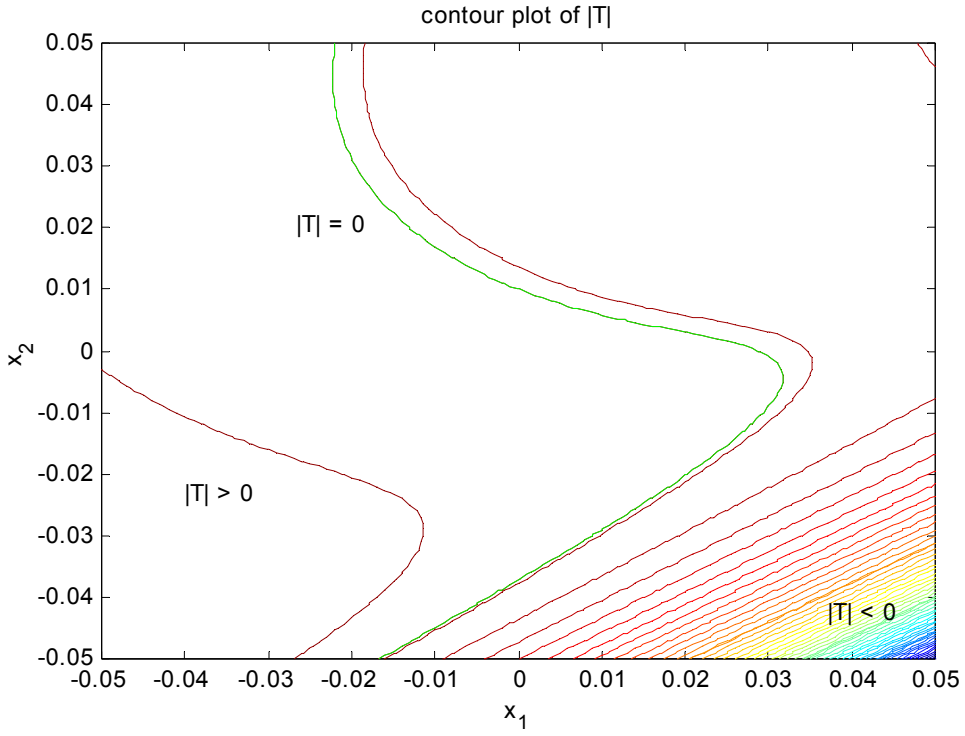

Figure 4.8 Contour plot of |T| to show noninvertible

Another way to look at this situation is as follows. Assuming a SISO 2nd order nonlinear system can be described by an input-output differential equation as $\ddot{q} = h(\dot{q}, q, \dot{u}, u, \theta)$, it can also be written in the form,

$$\begin{bmatrix} \dot{z}_1 \\ \dot{z}_2 \end{bmatrix} = \begin{bmatrix} z_2 \\ h(z_2, z_1, \ddot{u}, \dot{u}, u) \end{bmatrix} \tag{4.20}$$

where state variables $z_1 = q$ and $z_2 = \dot{q}$. Now for the small perturbation flame model that we discussed as in (4.16), the fundamental idea here is to verify if there is an invertible transformation between $[x_1 \quad x_2]^T$ and $[q \quad \dot{q}]^T$. If such a state transformation is invertible, it implies that there is a one to one correspondence between $[x_1 \quad x_2]^T$ and $[q \quad \dot{q}]^T$, and consequently (4.16) could be written in the form of equation (4.20), which essentially is the same as an input-output differential equation. The transformation between these two sets of variables is given in (4.18). Construct a matrix *T*,

$$T = \begin{bmatrix} \dfrac{\partial q}{\partial x_1} & \dfrac{\partial q}{\partial x_2} \\ \dfrac{\partial \dot{q}}{\partial x_1} & \dfrac{\partial \dot{q}}{\partial x_1} \end{bmatrix} \tag{4.21}$$

where,

$$\begin{aligned} \frac{\partial \dot{q}}{\partial x_1} &= \frac{\partial^2 q}{\partial x_1^2} f_1 + \frac{\partial q}{\partial x_1}\frac{\partial f_1}{\partial x_1} + \frac{\partial^2 q}{\partial x_1 \partial x_2} f_2 + \frac{\partial q}{\partial x_2}\frac{\partial f_2}{\partial x_1} \\ \frac{\partial \dot{q}}{\partial x_2} &= \frac{\partial^2 q}{\partial x_1 \partial x_2} f_1 + \frac{\partial q}{\partial x_1}\frac{\partial f_1}{\partial x_2} + \frac{\partial^2 q}{\partial x_2^2} f_2 + \frac{\partial q}{\partial x_2}\frac{\partial f_2}{\partial x_2} \end{aligned} \tag{4.22}$$

The sufficient condition for the existence of an invertible transformation is that the matrix *T* be invertible for all *u*. Figure 4.8 illustrates the determinant of matrix *T*. The green line denotes |*T*| = 0. Therefore, for certain values of $[x_1 \quad x_2]^T$, matrix *T* is not invertible. Consequently, there is likely no invertible transformation between $[x_1 \quad x_2]^T$ and

$[q \quad \dot{q}]^T$. This test is not as strong as the proceeding tests because it uses a sufficient condition, but it is easier to apply.

Thus we see that the state space model of Chapter 3 cannot be transformed into an input-output differential equation. For the case where the states of a system are known, but only input-output data are available, a recursive algorithm is developed in the section 4.4.1.

4.3 A Nonparametric System Identification Technique in the Frequency Domain

Frequency domain identification is widely used in linear system identification to estimate transfer functions. Given an input and output sequence, the correlation method or spectral analysis is applied to estimate the system frequency response [Lju99]. For nonlinear identification in the frequency domain, past work has been concerned mainly with static nonlinearities. Bendat developed a correlation technique using random data to identify up to third-order polynomial nonlinear models consisting of a linear system cascaded with a square law or cubic system [Ben90]. Yasuda et al presented a frequency domain technique to identify a two-dimensional vibrating elastic structure with geometric nonlinearity. Sinusoidal external force is applied at certain grid points, and the modal deflection is measured at others. Therefore the states for each modal equation are measured, and used to solve for unknown coefficients [Yas89]. This is different from our problem where the state variables are not observable.

In this section, we propose a nonparametric frequency domain identification technique, with input-output data only, based on the principle of harmonic balance. In this technique, the form of nonlinearity is unknown, and the states variables are not measurable. A pure sinusoidal signal with constant amplitude A and frequency ω is input to the nonlinear system, $u = A\sin(\omega t)$. After reaching steady state, the output wave shape can be represented by its Fourier series,

$$O(t) = \frac{A_0}{2} + A_1\cos(\omega t) + B_1\sin(\omega t) + A_2\cos(2\omega t) + B_2\sin(2\omega t) + \cdots \quad (4.23)$$

The decomposition of each frequency component of the output term results in,

$$\begin{aligned} f_1(t) &= A_1\cos(\omega t) + B_1\sin(\omega t) = F\sin(\omega t + \phi) \\ f_2(t) &= A_2\cos(2\omega t) + B_2\sin(2\omega t) = F_2\sin(2\omega t + \phi_2) \\ &\cdots \end{aligned} \quad (4.24)$$

With a small enough input amplitude A, the fundamental output component gain is just the linear frequency response. Increasing the input amplitude A results in nonlinear effects and output harmonics begin to show up. The fundamental component of the can be written as,

$$f_1(t) = F(A,\omega)\sin[\omega t + \phi(A,\omega)] \tag{4.25}$$

From a describing function viewpoint, the describing function magnitude and phase can be represented as $\frac{F(A,\omega)}{A}$ and $\angle\phi(A,\omega)$. We can easily consider higher harmonics of the output if the identification process requires. As the input amplitude A increases, the fundamental output magnitude and phase changes reflect odd nonlinearity, and the 2nd harmonic output is due to even nonlinearities. As an initial step of identification, small perturbations are used to determine the linear FRF, from which the order of system n can be found.

4.3.1 Harmonic Balancing for Nonparametric System Identifications

Based on linear estimation of the order of the model, we can tentatively model the system as an nth order differential equation. For example, a 4th order model with u as input and q as output can be written as,

$$\frac{d^4q}{dt^4} = f(\dddot{q},\ddot{q},\dot{q},q,\dddot{u},\ddot{u},\dot{u},u) \tag{4.26}$$

Different sets of data are needed with various input amplitudes and sweeping all the important frequencies. To simplify the description, we assume that only the fundamental output component is dominant in the output spectrum, which is true in the experimental results for our flame system. If the identified model has a poor fit with experimental data, consideration of both the fundamental and the 2nd harmonics in the balancing equation may be necessary.

Since we are only interested in the response at the fundamental frequency, quadratic terms are ignored and we assume that only cubic terms are important. For any input $u = A\sin(\omega_i t)$, the components of the fundamental frequency ω_i on both sides of the equation (4.26) should be balanced. Assuming the nonlinearity can be represented using *N* basis functions

$$\frac{d^4 q}{dt^4} = \sum_{i=1}^{N} p_i f_i(\dddot{q}, \ddot{q}, \dot{q}, q, \dddot{u}, \ddot{u}, \dot{u}, u), \tag{4.27}$$

each term on the right-hand side will contribute a $\sin(\omega_i t)$ term with amplitude designated as $f_{is}(\omega_i)$ and a $\cos(\omega_i t)$ term with amplitude $f_{ic}(\omega_i)$. The measured output $q = F(A, \omega_i)\sin[\omega_i t + \phi(A, \omega_i)]$ also can be decomposed into $\sin(\omega_i t)$ and $\cos(\omega_i t)$ terms. Harmonic balancing results in the matrix

$$\begin{array}{l}
\sin(\omega_1 t): \\
\cos(\omega_1 t): \\
\sin(\omega_2 t): \\
\cos(\omega_2 t): \\
\vdots \\
\sin(\omega_n t): \\
\cos(\omega_n t):
\end{array}
\begin{bmatrix}
f_{1s}(\omega_1) & f_{2s}(\omega_1) & f_{3s}(\omega_1) & \cdots & f_{Ns}(\omega_1) \\
f_{1c}(\omega_1) & f_{2c}(\omega_1) & f_{3c}(\omega_1) & \cdots & f_{Nc}(\omega_1) \\
f_{1s}(\omega_2) & f_{2s}(\omega_2) & f_{3s}(\omega_2) & \cdots & f_{Ns}(\omega_2) \\
f_{1c}(\omega_2) & f_{2c}(\omega_2) & f_{3c}(\omega_2) & \cdots & f_{Nc}(\omega_2) \\
\vdots & \vdots & \vdots & \vdots & \vdots \\
f_{1s}(\omega_n) & f_{2s}(\omega_n) & f_{3s}(\omega_n) & \cdots & f_{Ns}(\omega_n) \\
f_{1c}(\omega_n) & f_{2c}(\omega_n) & f_{3c}(\omega_n) & \cdots & f_{Nc}(\omega_n)
\end{bmatrix}
\begin{bmatrix} p_1 \\ p_2 \\ p_3 \\ \vdots \\ p_N \end{bmatrix} =
\begin{bmatrix}
-F_1\omega_1^4\cos(\phi_1) \\
-F_1\omega_1^4\sin(\phi_1) \\
-F_2\omega_2^4\cos(\phi_2) \\
-F_2\omega_2^4\sin(\phi_2) \\
\vdots \\
-F_n\omega_n^4\cos(\phi_n) \\
-F_n\omega_n^4\cos(\phi_n)
\end{bmatrix} \tag{4.28}$$

Concatenating the matrices for each set of amplitude runs allows us to solve for the coefficients p_i using a weighted least squares (WLS) method.

The principle of harmonic balancing is to equalize all frequency components on both sides of the equation. Generally, it is a reasonable assumption that the overall system has low pass characteristics. Thus, only a finite number of harmonics are important, and all higher order harmonics are negligible. Now, we discuss the most complicated case, where the effects of multiple harmonics are considered. To simplify the algebraic

computations, we express the principle of harmonic balancing in complex form rather than real form. Let input $u = \frac{1}{2}(Ae^{i\omega t} + \overline{A}e^{-i\omega t})$. The output q is expanded with complex amplitudes Q_i as

$$q = Q_0 + \frac{1}{2}(Q_1 e^{i\omega t} + \overline{Q}_1 e^{-i\omega t} + Q_2 e^{2i\omega t} + \overline{Q}_2 e^{-2i\omega t} + Q_3 e^{3i\omega t} + \overline{Q}_3 e^{-3i\omega t} + \cdots) \quad (4.29)$$

If only up to 3rd harmonics are retained, all the derivative terms and nonlinear terms can also be expanded into complex form easily. For example, the q^3 term is expanded as

$$\begin{aligned}
q^3 = {} & \frac{3}{8} e^{-8 i t w} \overline{Q_2}\, \overline{Q_3}^2 + \frac{1}{8} e^{-9 i t w} \overline{Q_3}^3 + e^{-7 i t w}\left(\frac{3}{8} \overline{Q_2}^2 Q_3 + \frac{3}{8} \overline{Q_1}\, \overline{Q_3}^2\right) + Q_0^3 + e^{-6 i t w}\left(\frac{\overline{Q_2}^3}{8} + \frac{3}{4} \overline{Q_1}\, \overline{Q_2}\, \overline{Q_3} + \frac{3}{4} \overline{Q_3}^2 Q_0\right) + \\
& \frac{3}{2} \overline{Q_1} Q_0 Q_1 + \frac{3}{8} \overline{Q_2} Q_1^2 + e^{-5 i t w}\left(\frac{3}{8} \overline{Q_1}\, \overline{Q_2}^2 + \frac{3}{8} \overline{Q_1}^2 Q_3 + \frac{3}{2} \overline{Q_2}\, \overline{Q_3} Q_0 + \frac{3}{8} \overline{Q_3}^2 Q_1\right) + \frac{3}{8} \overline{Q_1}^2 Q_2 + \frac{3}{2} \overline{Q_2} Q_0 Q_2 + \frac{3}{4} \overline{Q_3} Q_1 Q_2 + \\
& e^{-4 i t w}\left(\frac{3}{8} \overline{Q_1}^2 \overline{Q_2} + \frac{3}{4} \overline{Q_2}^2 Q_0 + \frac{3}{2} \overline{Q_1}\, \overline{Q_3} Q_0 + \frac{3}{4} \overline{Q_2}\, \overline{Q_3} Q_1 + \frac{3}{8} \overline{Q_3}^2 Q_2\right) + \frac{3}{4} \overline{Q_1}\, \overline{Q_2} Q_3 + \frac{3}{2} \overline{Q_3} Q_0 Q_3 + \frac{3}{8} e^{8 i t w} Q_2 Q_3^2 + \\
& \frac{1}{8} e^{9 i t w} Q_3^3 + e^{-i t w}\left(\frac{3}{2} \overline{Q_1} Q_0^2 + \frac{3}{8} \overline{Q_1}^2 Q_1 + \frac{3}{2} \overline{Q_2} Q_0 Q_1 + \frac{3}{8} \overline{Q_3} Q_1^2 + \frac{3}{4} \overline{Q_1}\, \overline{Q_2} Q_2 + \frac{3}{2} \overline{Q_3} Q_0 Q_2 + \frac{3}{8} \overline{Q_2}^2 Q_3 + \frac{3}{4} \overline{Q_1}\, \overline{Q_3} Q_3\right) + \\
& e^{-2 i t w}\left(\frac{3}{4} \overline{Q_1}^2 Q_0 + \frac{3}{2} \overline{Q_2} Q_0^2 + \frac{3}{4} \overline{Q_1}\, \overline{Q_2} Q_1 + \frac{3}{2} \overline{Q_3} Q_0 Q_1 + \frac{3}{8} \overline{Q_2}^2 Q_2 + \frac{3}{4} \overline{Q_1}\, \overline{Q_3} Q_2 + \frac{3}{4} \overline{Q_2}\, \overline{Q_3} Q_3\right) + \\
& e^{-3 i t w}\left(\frac{\overline{Q_1}^3}{8} + \frac{3}{2} \overline{Q_1}\, \overline{Q_2} Q_0 + \frac{3}{2} \overline{Q_3} Q_0^2 + \frac{3}{8} \overline{Q_2}^2 Q_1 + \frac{3}{4} \overline{Q_1}\, \overline{Q_3} Q_1 + \frac{3}{4} \overline{Q_2}\, \overline{Q_3} Q_2 + \frac{3}{8} \overline{Q_3}^2 Q_3\right) + \\
& e^{i t w}\left(\frac{3}{2} Q_0^2 Q_1 + \frac{3}{8} \overline{Q_1} Q_1^2 + \frac{3}{2} \overline{Q_1} Q_0 Q_2 + \frac{3}{4} \overline{Q_2} Q_1 Q_2 + \frac{3}{8} \overline{Q_3} Q_2^2 + \frac{3}{8} \overline{Q_1}^2 Q_3 + \frac{3}{2} \overline{Q_2} Q_0 Q_3 + \frac{3}{4} \overline{Q_3} Q_1 Q_3\right) + \\
& e^{2 i t w}\left(\frac{3}{4} Q_0 Q_1^2 + \frac{3}{2} Q_0^2 Q_2 + \frac{3}{4} \overline{Q_1} Q_1 Q_2 + \frac{3}{8} \overline{Q_2} Q_2^2 + \frac{3}{2} \overline{Q_1} Q_0 Q_3 + \frac{3}{4} \overline{Q_2} Q_1 Q_3 + \frac{3}{4} \overline{Q_3} Q_2 Q_3\right) + \\
& e^{5 i t w}\left(\frac{3}{8} Q_1 Q_2^2 + \frac{3}{8} Q_1^2 Q_3 + \frac{3}{2} Q_0 Q_2 Q_3 + \frac{3}{8} \overline{Q_1} Q_3^2\right) + e^{4 i t w}\left(\frac{3}{8} Q_1^2 Q_2 + \frac{3}{4} Q_0 Q_2^2 + \frac{3}{2} Q_0 Q_1 Q_3 + \frac{3}{4} \overline{Q_1} Q_2 Q_3 + \frac{3}{8} \overline{Q_2} Q_3^2\right) + \\
& e^{3 i t w}\left(\frac{Q_1^3}{8} + \frac{3}{2} Q_0 Q_1 Q_2 + \frac{3}{8} \overline{Q_1} Q_2^2 + \frac{3}{2} Q_0^2 Q_3 + \frac{3}{4} \overline{Q_1} Q_1 Q_3 + \frac{3}{4} \overline{Q_2} Q_2 Q_3 + \frac{3}{8} \overline{Q_3} Q_3^2\right) + e^{6 i t w}\left(\frac{Q_2^3}{8} + \frac{3}{4} Q_1 Q_2 Q_3 + \frac{3}{4} Q_0 Q_3^2\right) + \\
& e^{7 i t w}\left(\frac{3}{8} Q_2^2 Q_3 + \frac{3}{8} Q_1 Q_3^2\right)
\end{aligned} \quad (4.30)$$

Since we are only interested in the first 3 harmonics, only nonlinear terms up to $e^{3i\omega t} + cc$ are retained. The principle of harmonic balancing is then applied to terms of the form $e^{i\omega t}, e^{2i\omega t}, e^{3i\omega t}$ individually. In contrast to the real form in equation (4.28), the complex form expressions are separated into real and imaginary parts instead of $sin(\omega t)$ and $cos(\omega t)$ parts. Using a least squares method, all linear and nonlinear coefficients can be

obtained. The advantage of the complex form is the ease of using symbolic manipulation programs to compute the necessary harmonic terms.

In summary, a frequency domain nonparametric system identification technique is proposed from the principle of harmonic balancing. Both real and complex formulations were presented. Using a basis function approximation of the unknown nonlinearity, all coefficients are computed to find the best balance of output frequency components in a least squares sense.

4.3.2 Limitations of the Approach

There are some limitations of the above approach. First of all, the frequency response data covers such a small part of the state space that it only models the system response for sinusoidal input. Meanwhile, the input signal may not be a pure sinusoid due to physical constraints or feedback from the output. To identify the nonlinear heat release model, we would like to give a perturbation to the input velocity that is a pure sinusoid. But due to the coupling of combustor acoustics, the input velocity always contains harmonic components from output feedback. Nonetheless, we can still perform harmonic balancing by considering both input and output harmonics. This surely increases the complexity of the formulation. Moreover, it brings up the question of the number of harmonics that should be retained during the identification process.

Secondly, this approach does not enforce the stability of the nonlinear model. There is no guarantee that the identified nonlinear model is stable over the required operation range. Even though the identified model may fit the experimental data in the frequency domain, it does not guarantee stability of that particular steady state output solution. Suppose a nonlinear system with a sinusoidal perturbation $u = A\sin(\omega t)$ has a fundamental output $q = B\sin(\omega t + \phi)$ that matches the differential equation. If this periodic solution is not stable, it will not be found while conducting numerical simulation in forward time. This is similar to the theory of unstable limit cycles. Since the goal of the identified model is to reproduce all of the experimental data in digital simulations, the

stability has to be studied to be sure that the identified nonlinear model is stable over the required operational range.

Third, notice that amplitude and phase of output components were obtained from spectrum analysis of steady state output data. Since our experimental data are limited within certain amplitude and frequency ranges, the data only covers a subset of all possible frequencies and amplitudes of the input signal. Therefore, the transient response of the identified model should be considered cautiously, because the spectrum of transient response could be out of the frequency range of our experimental data. For a lightly damped system, output overshoot should be considered when studing the stability of the nonlinear model. Even though an identified model is stable within the experimental range of input-output data, the transient response may drive it out of the stability region and produce an unstable response. Since the transient is mainly due to the linear system response, we can estimate the transient from the identified linear model. Additionally, if the nonlinearity is approximated by polynomials, the model should be treated cautiously near the boundaries, because polynomials introduce large errors near the ends of the approximation zone.

4.4 Examples

Using the nonparametric identification algorithm that we proposed in the previous section, several practical examples are presented below to illustrate the procedures and improvements. First, a simple low order nonlinear model is constructed from experimental data measured from a flat flame burner. To avoid the difficulties and limitation of higher-order models that we discussed earlier, a subsystem modeling method is also used to provide a better solution for this complicated system. Next, the technique is generalized to handle the identification of a nonlinear state space model, where the states are specified by a linear model. As an example, the technique is applied to a Hammerstein-Weiner model with static nonlinearity at the input and output.

4.4.1 Example of Nonlinear Identification from Experiments

In this section, we will present an example of nonlinear system identification from experimental data with the frequency domain nonparametric identification technique that we developed. Experimental data is collected for a laminar premixed flame burner, and a nonlinear heat release model is constructed from velocity perturbation u' of incoming fuel air mixture to the output heat release rate q'. Premixed fuel-air mixture with constant equivalence ratio ϕ flows through the combustor at mean velocity u_0. The acoustic velocity perturbation u' is generated by a side-mounted speaker. A velocity sensor is placed just below the flame holder to measure the input sinusoid u' and a PMT OH* sensor is placed above the flame to measure the heat release rate q'. The input velocity is increased from small to large by raising the voltage applied to the speaker. With the speaker voltage set small enough, the measured system response is close to linear, and the output heat release rate magnitude and phase over the input velocity gives the linear FRF. To identify the nonlinear system, the speaker voltage has to be raised high enough to reveal the effect of nonlinearity.

Ideally, we would like to conduct an experiment with a pure sinusoidal input and measure the output fundamental and harmonics. For the experiment, a sinusoid voltage source is applied to the speaker at each frequency within a bandwidth of 20-380Hz. The speaker voltage amplitude was held constant at various levels, and the input velocity u' in conjunction with the output heat release rate response q' was measured as a function of frequency. Due to the speaker dynamics and the effect of the acoustic dynamics of the combustor itself, the input velocity will not have constant amplitude at all frequencies. Figure 4.9 shows the velocity amplitudes measured at each speaker voltage as a function of frequency. Meanwhile, the experiment shows that both input u' and output q' have relatively small harmonics compared to the fundamental magnitude. So, we are only interested in the fundamental magnitude and phase response, which is analogous to describing functions. The experimental measurements of the frequency response function from input velocity u' to heat release rate q' at various speaker voltage levels are shown in Figure 4.10.

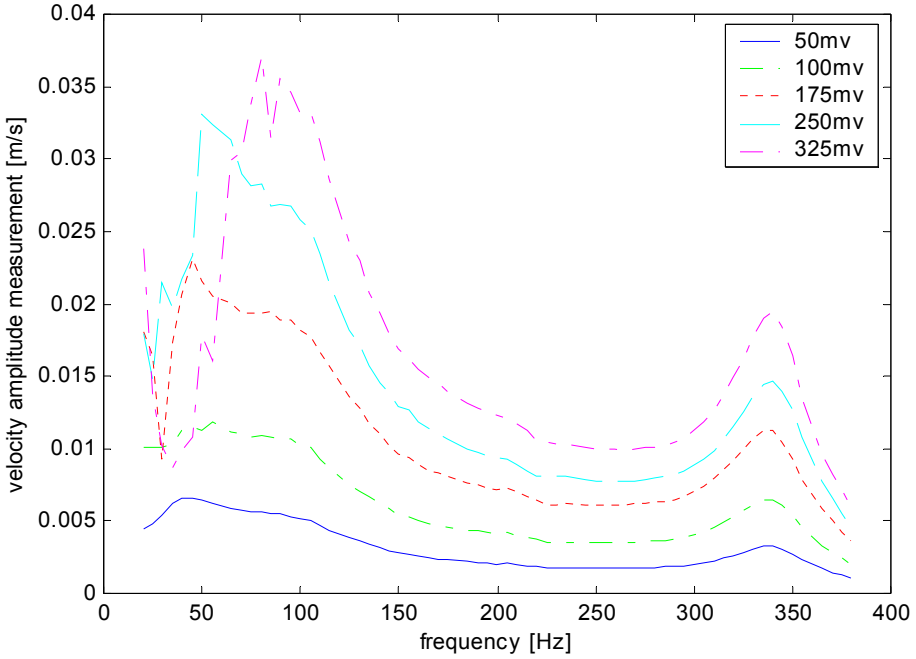

Figure 4.9 Velocity amplitude measured at different speaker voltage settings.

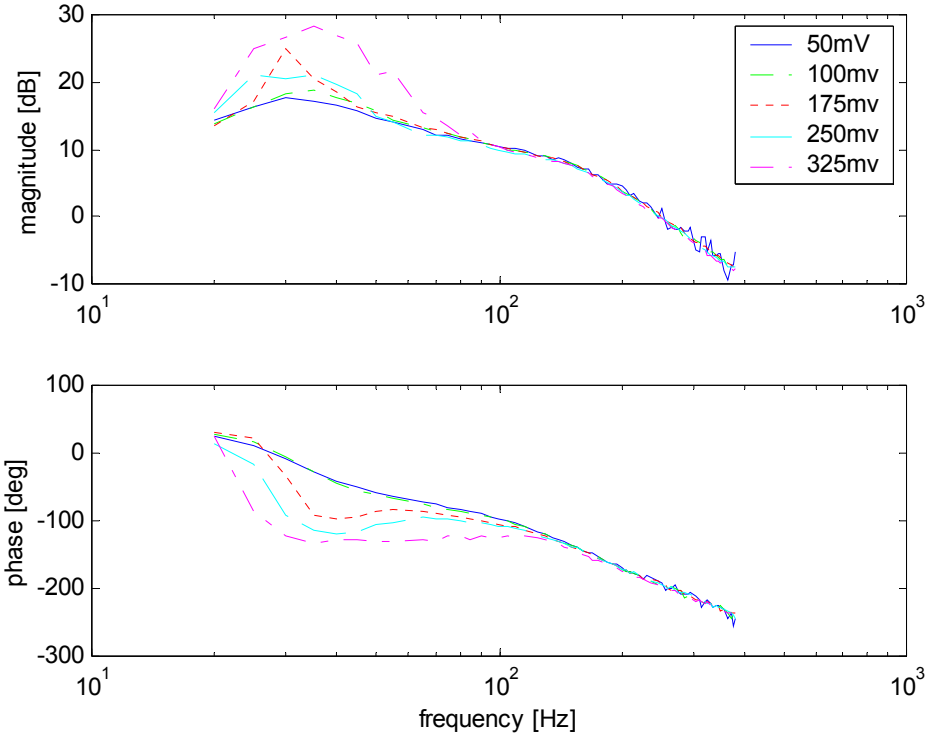

Figure 4.10 Experimental measurement of the velocity to heat release rate transfer function at various speaker voltage levels.

4.4.1.1 Working with Subsystems

From the frequency response functions generated by the small perturbation inputs, we can easily obtain the linear part of the model. In the data above, the 50mv and 100mv data sets disclosure the linear system response. Using an inverse frequency response technique gives a 4th order linearized model of the system with two pairs of complex conjugate poles at 32.7 Hz and 144.3 Hz, respectively. A comparison of the frequency response of the linearized model with the 50mv data is shown in Figure 4.11.

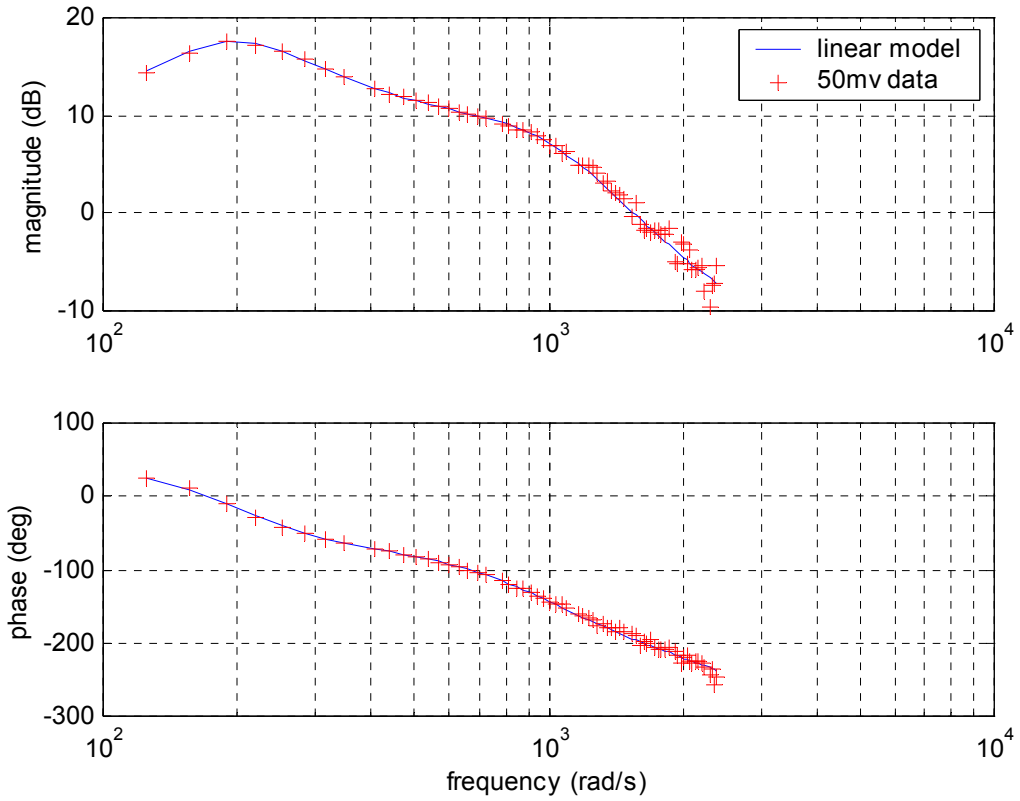

Figure 4.11 Comparison of identified linear part of model and 50mv data set

There is an immediate approach to model the nonlinear heat release dynamics into a 4th order differential equation with a set of cubic terms as

$$\frac{d^4 q}{dt^4} = f(\dddot{q}, \ddot{q}, \dot{q}, q, \frac{d^4 u}{dt^4}, \dddot{u}, \ddot{u}, \dot{u}, u) \tag{4.31}$$

With 9 linear terms and 24 nonlinear cubic terms, a model as in (4.31) is constructed and it fits the data in Figure 4.10. An example for speaker voltage at 325mV is shown in Figure 4.12 below. Indeed, with a large number of nonlinear terms and choosing a proper weighting function, it is easy to find a model that fits the experimental data. However this 4^{th} order model is only stable within a narrow region close to the initial steady state. Therefore it could reproduce the 50mv and 100mv data sets, but when the excitation got larger, this model became unstable and the simulation diverged. For this 9 dimensional system, the experimental data can only cover a very small subset of this high-dimensional space. Once the transient moves out of that small subset, the behavior of the nonlinear model is not defined, and it could go unstable. Moreover, there are too many nonlinear terms available to approximate the unknown nonlinearity. Thus, we developed a subsystem modeling technique to obtain better identifications and alleviate stability concerns.

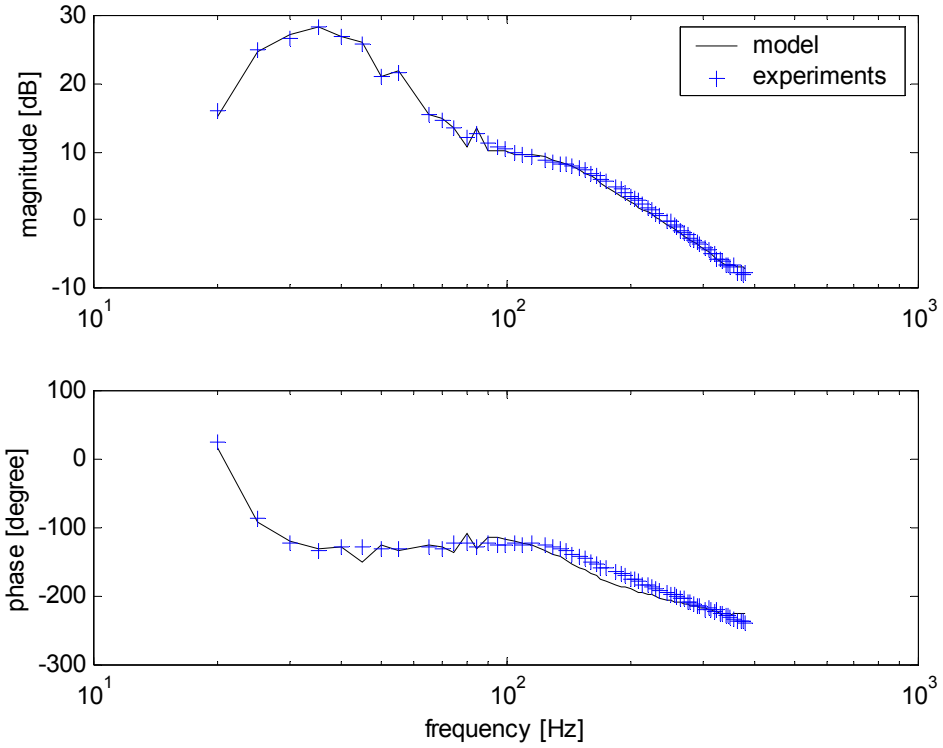

Figure 4.12 Comparison of 4^{th} order model with experimental data set of speaker voltage 325mv

As we can see from the experimental data shown in Figure 4.10, significant nonlinearity was measured in the low frequency range. While in the high frequency range, the data captured is mostly linear. So, the model to be identified must at least fit all the nonlinear frequency response data in the low frequency range. The 4th order linear model shown in Figure 4.13 can be separated into two 2nd order subsystems. With small contributions from subsystem 1, subsystem 2 captures the linear frequency response in the high frequency range.

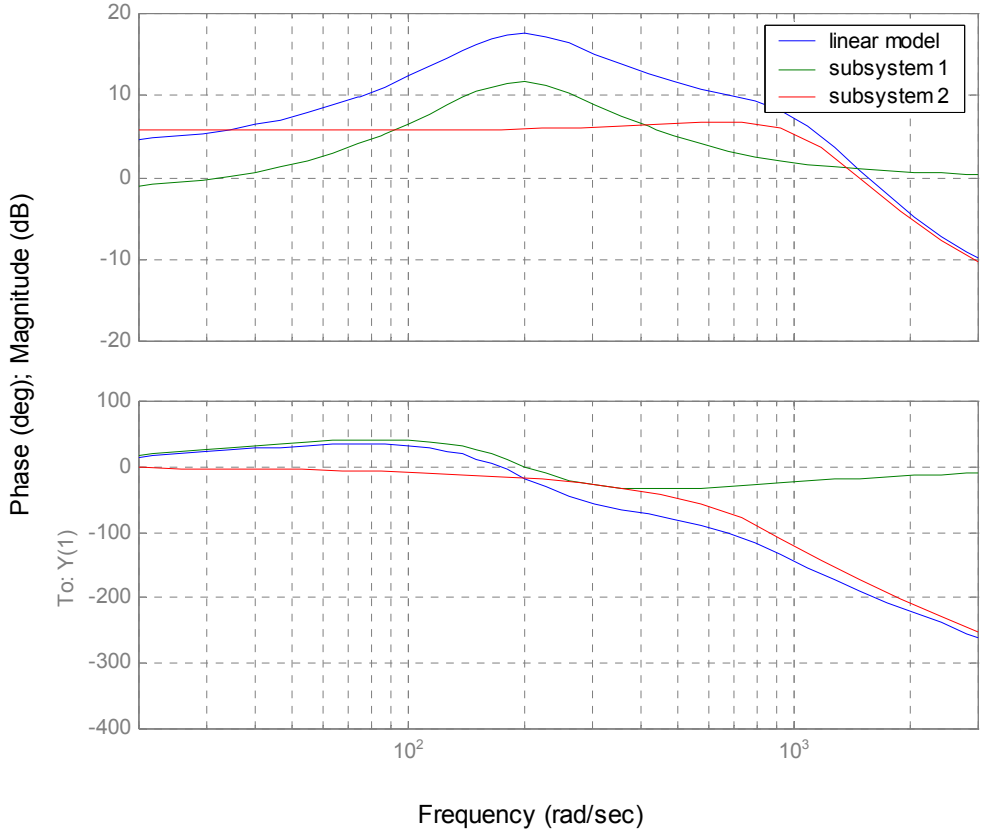

Figure 4.13 Frequency response of linear model and subsystems

A cascade structure is built from two 2nd order subsystems as shown in Figure 4.14. Since the experimental data contains nonlinear information only in the low frequency range, it

is assumed that subsystem1 contains all of the nonlinearity while subsystem2 is purely linear low pass filter.

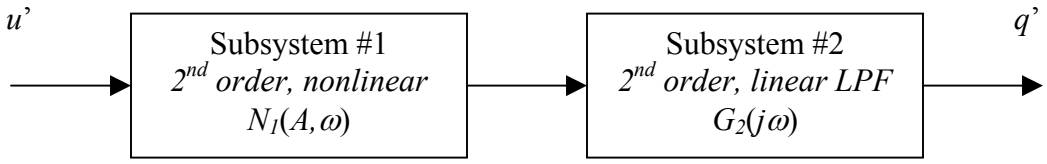

Figure 4.14 Scheme of cascade form with two 2nd order subsystems

There are various ways to break a 4th order linear model into two 2nd order models. The criteria is that subsystem 2 is selected to be a low pass or all pass filter so that it does not have significant low frequency dynamics. Since we are using only the fundamental frequency component of the nonlinear system, the order sequence for these two subsystems is not a problem. If the higher harmonics are considered, the order of the subsystems should be considered.

The advantage of this subsystem modeling approach is to preprocess the data and require only a 2nd order nonlinear model. It is relatively simple to study the stability of a 2nd order nonlinear model. Also, there are fewer nonlinear terms available to fit the measured data. Nonetheless, a disadvantage of this specific example is that the experimental data is linear in the high frequency range due to small input excitations, and thus the identified nonlinear model may not be accurate in predicting large-excitation nonlinear responses in the high frequency range.

4.4.1.2 Identifications of A Second Order Nonlinear Subsystem

Let the overall system frequency response be $F(A,\omega)$, and the linear subsystem 2 have linear FRF $G_2(j\omega)$. Therefore, the nonlinear data for nonlinear subsystem 1 $N_1(A,\omega)$ can be computed as,

$$N_1(A,\omega) = \frac{F(A,\omega)}{G_2(j\omega)}$$
$$|N_1(A,\omega)| = \frac{|F(A,\omega)|}{|G_2(j\omega)|}, \angle N_1(A,\omega) = \angle F(A,\omega) - \angle G_2(j\omega) \tag{4.32}$$

The magnitude response of subsystem 1 is equal to the experimental data magnitude value divided by the magnitude of $G_2(j\omega)$, and the phase is computed by subtracting the phase of $G2(j\omega)$ from the original phase values. Figure 4.15 shows the new data sets for identification of the nonlinear 2nd order subsystem. Since only the fundamental output is considered in this example, a model structure of a 2nd order linear system in conjunction with several cubic nonlinear terms is selected.

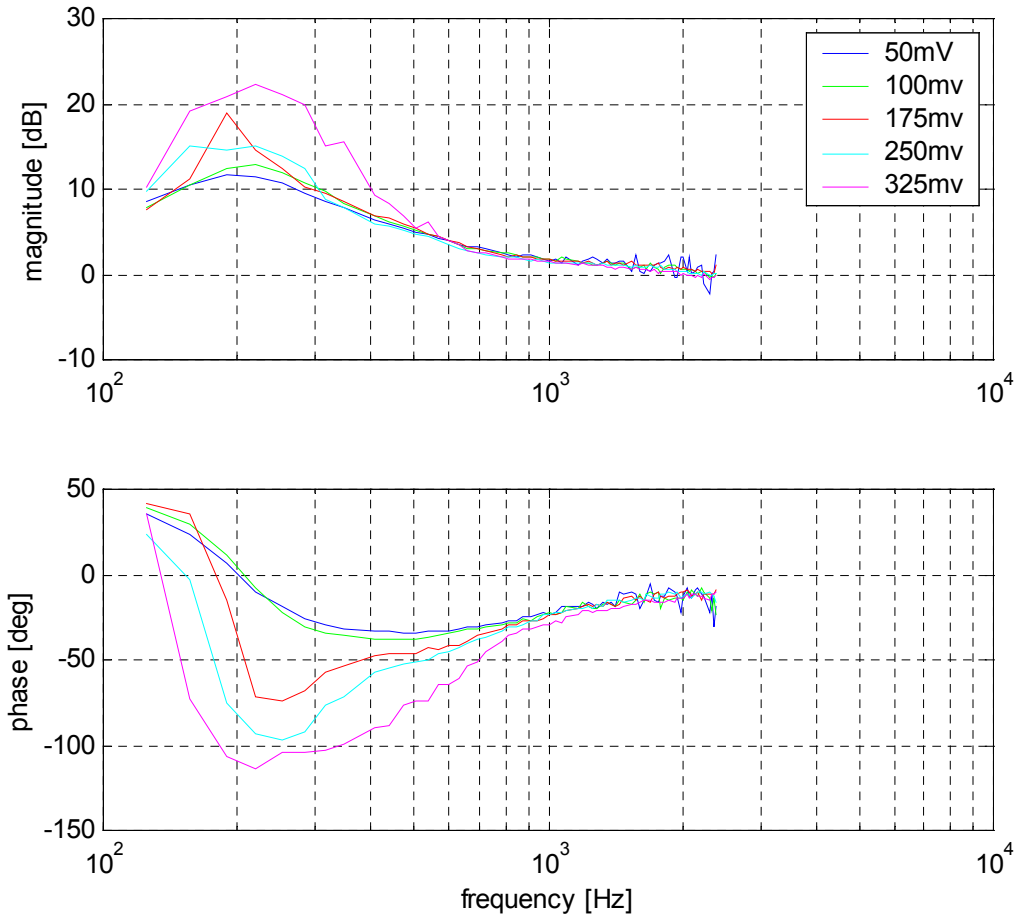

Figure 4.15 Preprocessed nonlinear data to be identified for subsystem 1.

To identify a 2nd order nonlinear model in the frequency domain with the technique that we developed earlier, assume the system is in the form of $\ddot{q} = f(\dot{q}, q, \ddot{u}, \dot{u}, u)$. If the input is a sinusoidal signal $u = A\cos(\omega t)$, and fundamental output is $q = B\cos(\omega t + \phi)$, so $\ddot{q} = -\omega^2 B\cos(\omega t + \phi) = -\omega^2 q$. If quantities are expressed in complex form, the least squares minimization goal is,

$$\min[(\hat{\ddot{q}}_r - \ddot{q}_r)^2 + (\hat{\ddot{q}}_i - \ddot{q}_i)^2] = \omega^4 \min[(\hat{q}_r - q_r)^2 + (\hat{q}_i - q_i)^2].$$

Clearly, the errors of data in the high frequency range are heavily weighted by ω^4. Therefore, a weighted least squares method is implemented with increased weight on the low frequency data. With a few cubic nonlinear terms, q^3, q^2u, qu^2, u^3, $\dot{q}u^2, \dot{q}qu, \dot{q}q^2, \dot{u}u^2, \dot{u}qu, \dot{u}q^2$, a model is identified and it fits the data well. An example of the identification result is shown in Figure 4.16 where the identified model is compared with the 325mv experimental data set. The model and data reaches good agreement.

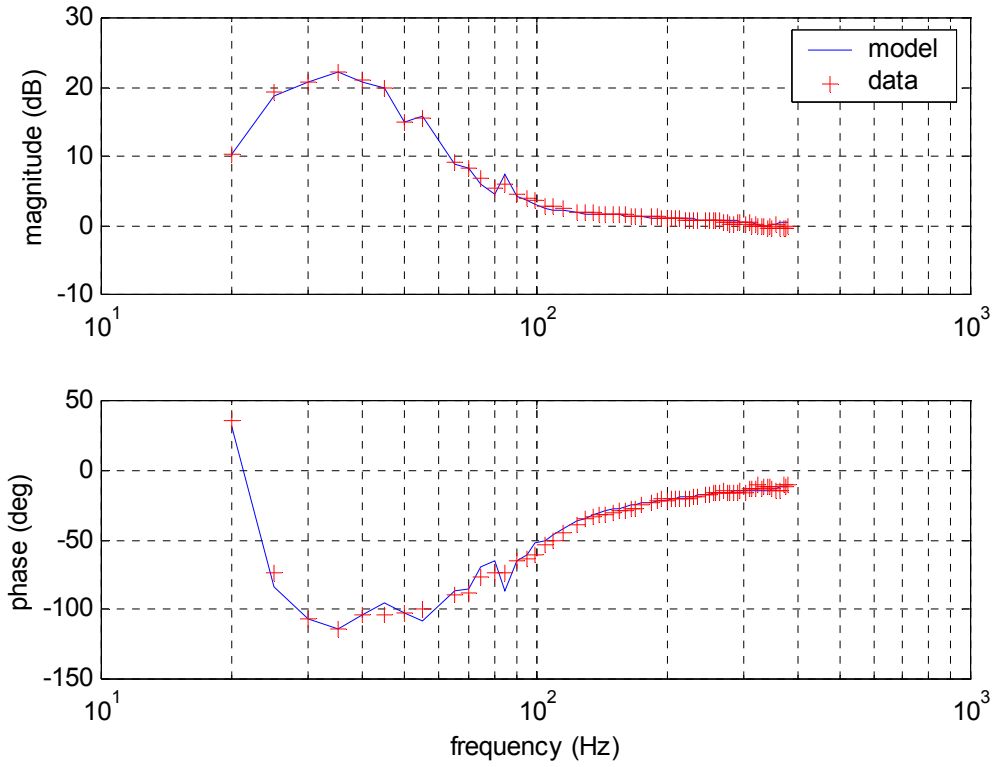

Figure 4.16 Comparison of identified model and 325mv experimental data

4.4.1.3 Discussion of model stability and validation

The nonlinear model stability should be guaranteed within the entire input-output range of the data so that the model is able to reproduce the original experimental data. The identified 2nd order nonlinear model can be described by,

$$\begin{aligned}\ddot{q} = {} & \theta_1\dot{q} + \theta_2 q + \theta_3\ddot{u} + \theta_4\dot{u} + \theta_5 u + \theta_6 q^3 + \theta_7 q^2 u + \theta_8 q u^2 + \theta_9 u^3 \\ & + \theta_{10}\dot{q}u^2 + \theta_{11}\dot{q}qu + \theta_{12}\dot{q}q^2 + \theta_{13}\dot{u}u2 + \theta_{14}\dot{u}qu + \theta_{15}\dot{u}q^2\end{aligned} \tag{4.33}$$

To find the equilibrium points and Jacobian matrices to assess stability, the model is written in state space form, where $x_1 = q,\ \ x_2 = \dot{q}$.

$$\begin{aligned}\dot{x}_1 &= x_2 \\ \dot{x}_2 &= \theta_1 x_2 + \theta_2 x_1 + \theta_6 x_1^3 + \theta_{12} x_2 x_1^2\end{aligned} \tag{4.34}$$

Setting $\dot{x}_1 = \dot{x}_2 = 0$, the fixed points are $x_1 = 0, \pm\sqrt{-\theta_2 / \theta_6}$, $x_2 = 0,0,0$. Stability can be determined by computing eigen values of the Jacobian matrix J at each fixed point.

$$J = \begin{bmatrix} 0 & 1 \\ \theta_2 + 3\theta_6 x_1^2 + 2\theta_{12} x_1 x_2 & \theta_1 + \theta_{12} x_1^2 \end{bmatrix} \tag{4.35}$$

With the given data, the identified model has a stable focus at the origin and two saddle points at $(\pm 0.625,0)$. Considering the output amplitude plot in Figure 4.17,it can be seen that all experimental data is within the stable range. Numerical simulations validate the identified model and it is able to reproduce all experimental data with a satisfactory accuracy. Furthermore, even though the experimental data does not contain nonlinear responses in the high frequency range, Figure 4.18 shows a nonlinear response at 175Hz with input amplitude 0.45. Thus, this model exhibits nonlinear responses in the high frequency range as well.

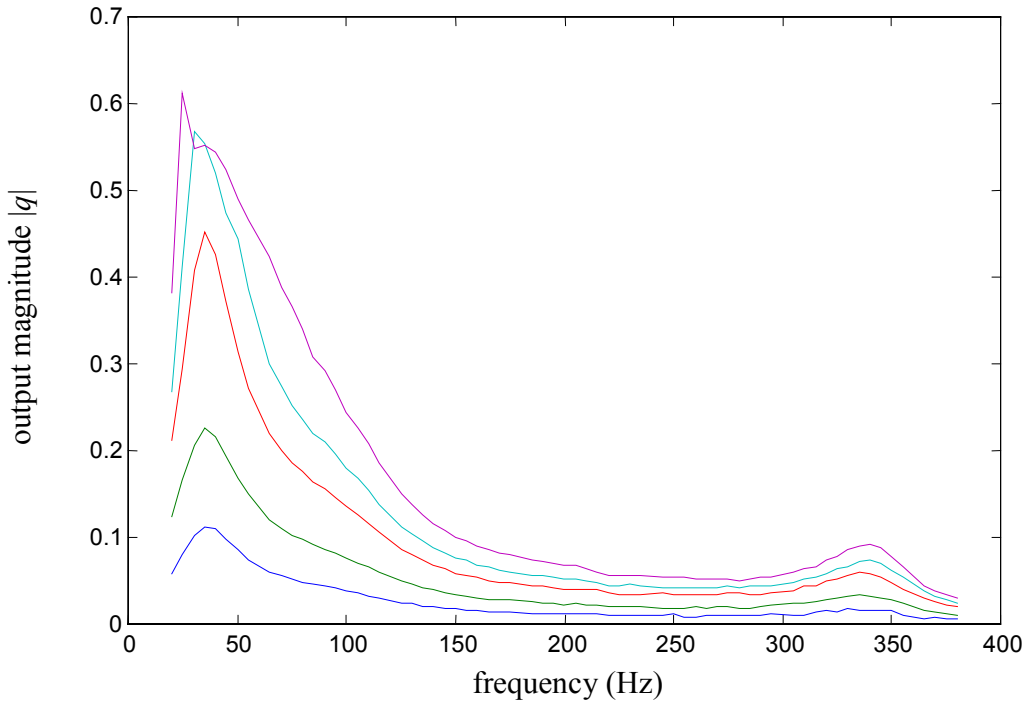

Figure 4.17 Output magnitude of the 2nd order nonlinear model

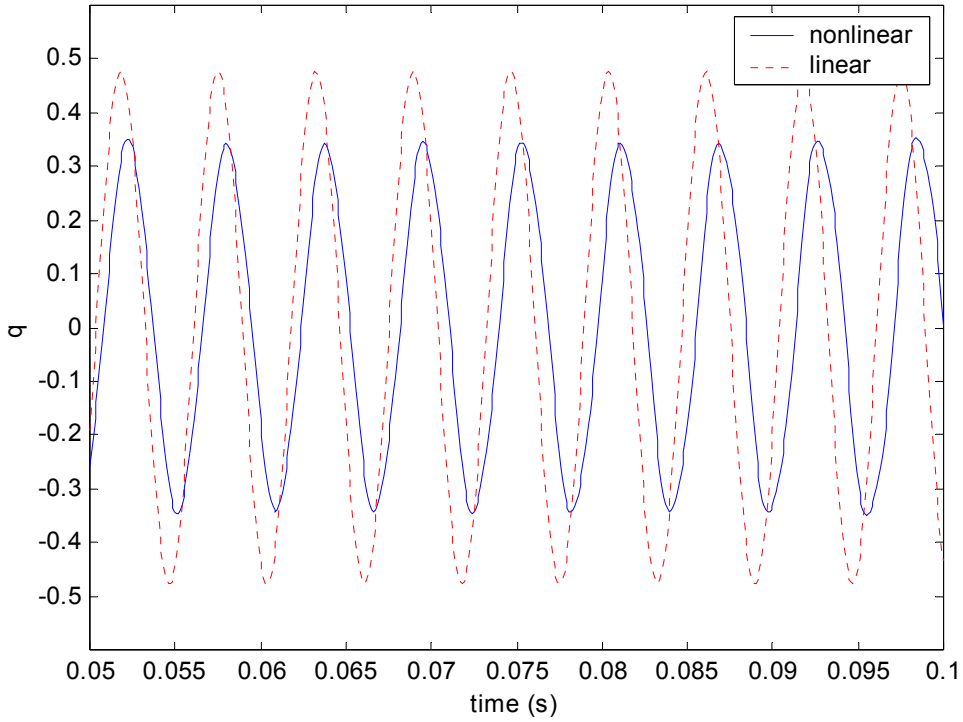

Figure 4.18 Simulation of model with input A = 0.5 at f = 175Hz

4.4.2 Example of State Space Model Identifications

A 2nd order nonlinear state space model is described as in equation (4.36), where θ and γ are vectors of unknown nonlinear coefficients and p and q are state variables.

$$\begin{bmatrix} \dot{p} \\ \dot{q} \end{bmatrix} = \begin{bmatrix} A_{11} & A_{12} \\ A_{21} & A_{22} \end{bmatrix} \begin{bmatrix} p \\ q \end{bmatrix} + \begin{bmatrix} b_1 \\ b_2 \end{bmatrix} u + \begin{bmatrix} \hat{f}_1(p,q,u,\theta) \\ \hat{f}_2(p,q,u,\theta) \end{bmatrix}$$
$$y = C \begin{bmatrix} p \\ q \end{bmatrix} + \hat{g}(p,q,\gamma) \tag{4.36}$$

It is assumed that: (1) the linear part of model is identified through small perturbations and transfer functions, so the system matrices $\{A, B, C\}$ are known; (2) the form of the nonlinearity in the state equations and the output equation can be modeled from physics or using polynomial expansions; (3) state variables p, q are not directly measurable. Only the input u and the output y are available.

4.4.2.1 An Identification Algorithm for a State Space Model

Suppose the input u, state variables p and q, and output y can be approximated using a Fourier series. We also assume, for simplicity, that only the first three harmonics are needed,

$$\begin{aligned} u &= \frac{1}{2}(A_1 e^{i\omega t} + \overline{A}_1 e^{-i\omega t}) = [A_1, \overline{A}_1] \\ p &= [P_1, \overline{P}_1, P_2, \overline{P}_2, P_3, \overline{P}_3 \cdots] \\ q &= [Q_1, \overline{Q}_1, Q_2, \overline{Q}_2, Q_3, \overline{Q}_3 \cdots] \\ y &= [y_1, \overline{y}_1, y_2, \overline{y}_2, y_3, \overline{y}_3 \cdots] \end{aligned} \tag{4.37}$$

Applying harmonic balancing to the state equations in (4.36), results in the set of equations,

$$\begin{aligned} j\omega P_1 &= f_1(A_1, P_1, P_2, P_3, Q_1, Q_2, Q_3, \theta) \\ 2j\omega P_2 &= f_2(A_1, P_1, P_2, P_3, Q_1, Q_2, Q_3, \theta) \\ 3j\omega P_3 &= f_3(A_1, P_1, P_2, P_3, Q_1, Q_2, Q_3, \theta) \\ j\omega Q_1 &= f_4(A_1, P_1, P_2, P_3, Q_1, Q_2, Q_3, \theta) \\ 2j\omega Q_1 &= f_5(A_1, P_1, P_2, P_3, Q_1, Q_2, Q_3, \theta) \\ 3j\omega Q_1 &= f_6(A_1, P_1, P_2, P_3, Q_1, Q_2, Q_3, \theta) \end{aligned} \tag{4.38}$$

And the output equation can be balanced as,

$$\begin{aligned} Y_1 &= g_1(Y_1, Y_2, Y_3, P_1, P_2, P_3, Q_1, Q_2, Q_3, \gamma) \\ Y_2 &= g_2(Y_1, Y_2, Y_3, P_1, P_2, P_3, Q_1, Q_2, Q_3, \gamma) \\ Y_3 &= g_3(Y_1, Y_2, Y_3, P_1, P_2, P_3, Q_1, Q_2, Q_3, \gamma) \end{aligned} \tag{4.39}$$

For each input-output data set at frequency ω_i, we have two sets of equations as in (4.38-39) with θ and γ as unknown coefficients, and $[P_1, P_2, P_3, Q_1, Q_2, Q_3]$ as intermediate variables. The goal is to find coefficients θ and γ to minimize the mean square error at all frequencies $\frac{1}{N}\sum_{i=1}^{N} err_i$, where for frequency ω_i,

$$err_i = (Y_{1i} - \hat{Y}_{1i})^2 + (Y_{2i} - \hat{Y}_{2i})^2 + (Y_{3i} - \hat{Y}_{3i})^2 \tag{4.40}$$

The iterative identification algorithm is as follows:

1. Apply sinusoidal inputs at the required frequencies and amplitudes, and obtain all harmonic components of the output $[Y_1, Y_2, Y_3]$.

2. Given an initial guess for θ, solve the coupled nonlinear equation set (4.38) to obtain all state variables $[\hat{P}_1, \hat{P}_2, \hat{P}_3, \hat{Q}_1, \hat{Q}_2, \hat{Q}_3]$.

3. Replace $[P_1, P_2, P_3, Q_1, Q_2, Q_3]$ with those computed $[\hat{P}_1, \hat{P}_2, \hat{P}_3, \hat{Q}_1, \hat{Q}_2, \hat{Q}_3]$ values in the right side of equation (4.38), and the left side of equation remains unchanged with $[P_1, P_2, P_3, Q_1, Q_2, Q_3]$ as variables. Now we can see that $P_1, P_2, P_3, Q_1, Q_2, Q_3$ each becomes a function of coefficients θ.

4. Substitute $P_1, P_2, P_3, Q_1, Q_2, Q_3$ with functions of θ in equation (4.39), and now each equation becomes $Y_i = g_i(Y_1, Y_2, Y_3, \theta, \gamma)$ which is essentially a traditional nonlinear regression problem. Use a nonlinear least squares or simplex search algorithm to update those unknown coefficients θ and γ to minimize err_i.

5. With the most recently updated θ and γ values, go back to step 2 to solve for a new set of state variables and repeat step 3 conversion and step 4 nonlinear regression process.

6. Repeat the process for each frequency ω_i, and reiterate the process with experimental data until the coefficients θ, γ converge and error of all data sets are minimized.

This iterative identification algorithm can be applied to standard state space nonlinear system identification problems. A simple example is presented in the next section with a Wiener-Hammerstein model.

4.4.2.2 An Example of Wiener-Hammerstein Identification

The term Wiener model normally refers to a system with a static nonlinearity at the output, while a Hammerstein model is defined as a linear system with a static nonlinearity at the input. Below we identify a nonlinear system with cubic nonlinearities at both the input and output. Figure 4.19 illustrates the structure of the nonlinear model.

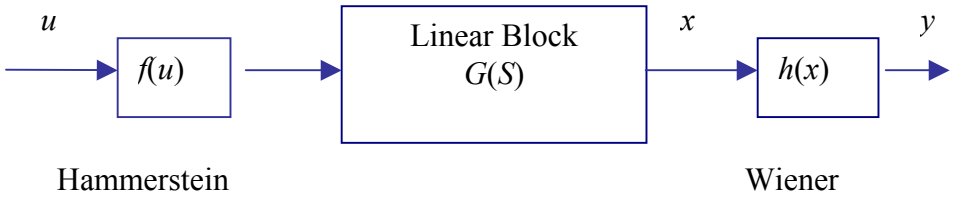

Figure 4.19 Block diagram of a Wiener-Hammerstein system

Assume the linear part of this 2nd order example model has been identified prior to this stage. The model structure is described as,

$$\begin{bmatrix}\dot{p}\\ \dot{q}\end{bmatrix}=\begin{bmatrix}A_{11} & A_{12}\\ A_{21} & A_{22}\end{bmatrix}\begin{bmatrix}p\\ q\end{bmatrix}+\begin{bmatrix}b_1\\ b_2\end{bmatrix}u+\begin{bmatrix}\alpha_1\\ \alpha_2\end{bmatrix}u^3$$
$$y=C\begin{bmatrix}p\\ q\end{bmatrix}+\begin{bmatrix}\beta_1 & \beta_2\end{bmatrix}\begin{bmatrix}p^3\\ q^3\end{bmatrix} \qquad (4.41)$$

Unknown coefficients $\alpha_1,\alpha_2,\beta_1,\beta_2$ are to be identified using the recursive algorithm that we developed earlier. With an example system,

$$A=\begin{bmatrix}-1 & -2\\ 2 & 0\end{bmatrix}\quad B=\begin{bmatrix}1\\ 0\end{bmatrix}\quad C=\begin{bmatrix}1 & 1\end{bmatrix}\quad \begin{bmatrix}\alpha_1\\ \alpha_2\end{bmatrix}=\begin{bmatrix}2\\ 3\end{bmatrix}\quad \begin{bmatrix}\beta_1 & \beta_2\end{bmatrix}=\begin{bmatrix}4 & 5\end{bmatrix}$$

It can be formulated as in equation (4.38-40) and the algorithm that we described earlier is applied with a simplex search routine for updating coefficients. Figure 4.20 shows the convergence of those 4 unknown coefficients. Starting from initial [1 1 1 1], it converged to the target values [2 3 4 5] after about 3000 iterations. Note that simplex search takes more iterations and computational time to obtain the result, but it has the advantage of avoiding local minimum. Figure 4.21 shows the output error surface as a function of the parameters $\alpha_1, \alpha_2, \beta_1, \beta_2$. Clearly it is parabolic in nature, and the optimal solutions are obtained from our identification algorithm.

In conclusion, for state space nonlinear model, system identification is not as straightforward as a single differential equation. But with a recursive identification algorithm that we developed above, nonlinear optimization process enables us to find the best set of coefficients to fit the data in frequency domain.

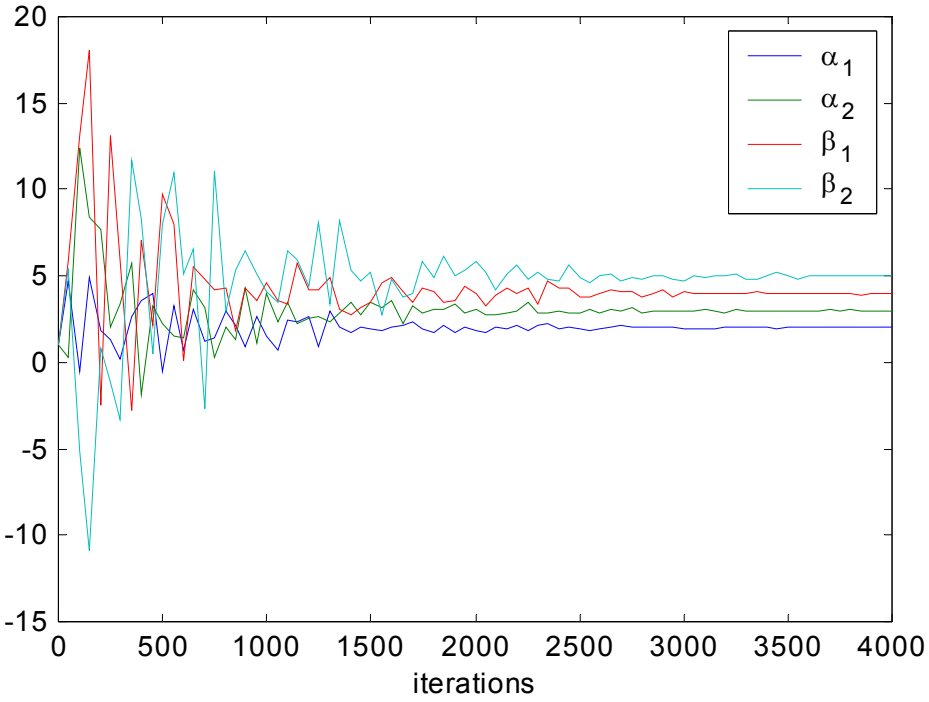

Figure 4.20 Parameter convergence of the Wiener-Hammerstein model

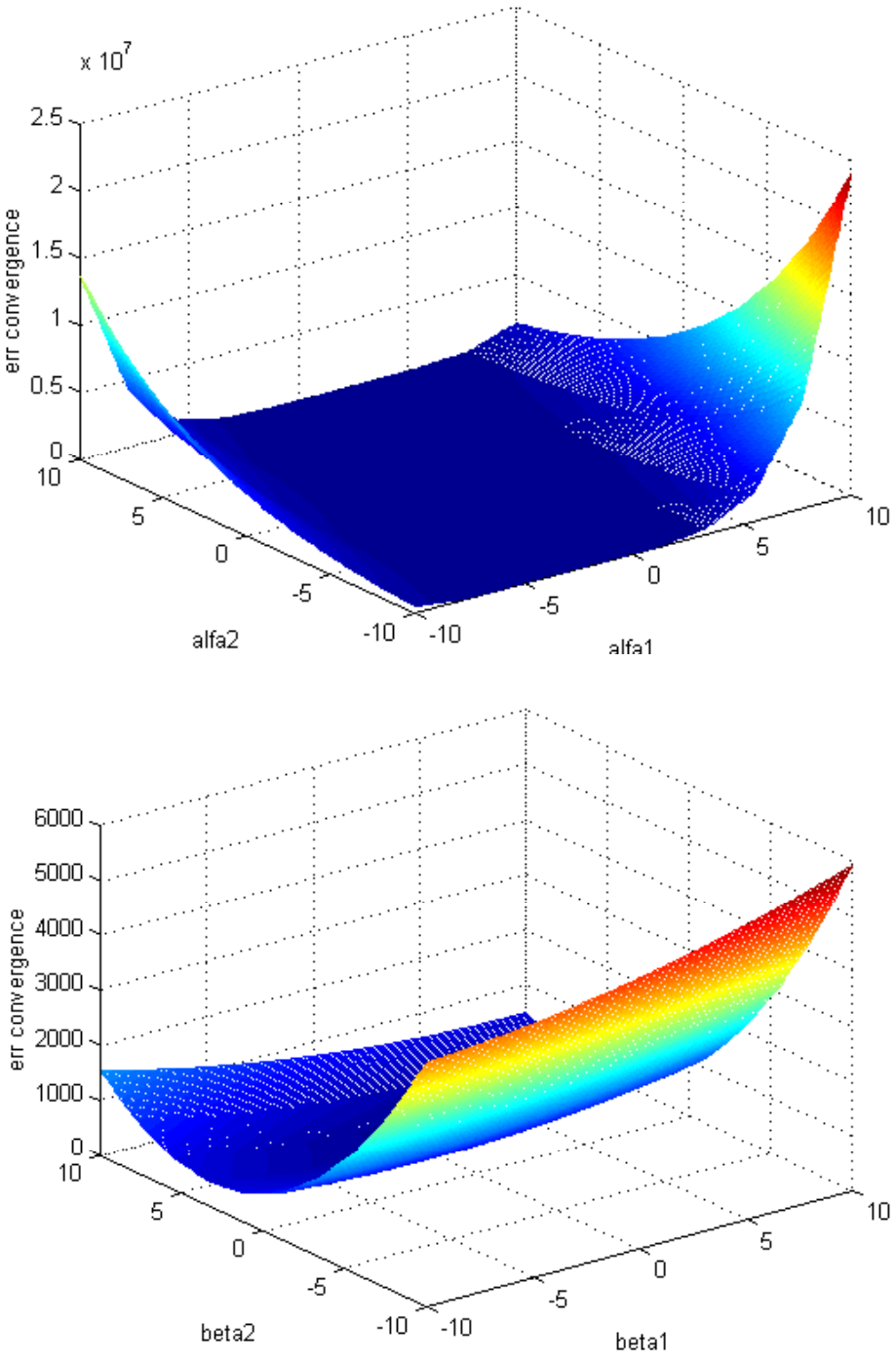

Figure 4.21 Error surface of an example 2nd order nonlinear model with unknown coefficients